

Abstracts of the Papers Published by the Staff Members of the Institute from July, 1977 to June, 1978

Nuclear Chemistry

Mesure de Très Grandes Résistances pour l'Isolation de Détecteurs de Radiations. R. Sellam, S. Kakiuchi, and H. Mazaki. *Bull. Inst. Chem. Res., Kyoto Univ.*, **56**, 1 (1978). — For precise measurements of very small ionization current ($10^{-10} \sim 10^{-16}$ A) by nuclear radiations, a method of extremely high insulation test (up to $10^{18} \Omega$) is proposed. Applying the test for teflon $(CF_2CF_2)_n$, electrical resistances of the order of $10^{15} \sim 10^{18} \Omega$ can be measured within inaccuracy of $\pm 5 \sim \pm 30\%$.

A Monte-Carlo Method for Calculations of the Distribution of Angular Deflections due to Multiple Scattering. T. Mukoyama and Y. Watanabe. *Bull. Inst. Chem. Res., Kyoto Univ.*, **56**, 6 (1978). — A Monte Carlo method for calculation of the distribution of angular deflections of fast charged particles passing through thin layer of matter is described on the basis of Molière theory of multiple scattering. The distribution of the angular deflections obtained as the result of calculations is compared with Molière theory. The method proposed is useful to calculate the electron transport in matter by Monte Carlo method.

Positron Production in Superheavy Ion-Atom Collision Systems. H. Backe, E. Berdermann, H. Bokemeyer, J. S. Greenberg, E. Kankeleit, P. Kienle, Ch. Kozhuharov, L. Handschug, Y. Nakayama, L. Richter, H. Stettmeier, F. Weik, and R. Willwater. *Proceedings of the 10th International Conference on the Physics of Electronic and Atomic Collision, Paris, 7 (1977) (Commissariat à l'Énergie Atomique, Paris, 1977, p. 162)*. — Experiments have been initiated to investigate positron creation induced in the collision between very heavy atoms. In particular, the investigations are focussing on the isolation of the processes leading to direct positron production in the Coulomb fields of the colliding systems, and induced and spontaneous emission in overcritical electric fields. Both total cross sections and differential cross sections with respect to the scattered ions are being explored, utilizing two instruments possessing somewhat complementary features of positron detection and background suppression.

In-Beam Spectroscopy of Low Energy Conversion Electrons with a Recoil Shadow Method — A New Possibility for Subnanosecond Lifetime Measurements. H. Backe, L. Richter, R. Willwater, E. Kankeleit, Y. Nakayama, and B. Martin. *Zeit. f. Phys., A*, **285**, 159 (1978). — An electron spectrometer consisting of an electron transport system with normal conducting solenoidal coils and a Si(Li)-detector as the energy dispersive element is described. It can be used for in beam spectroscopy of electrons in three different modes. The first one is the usual broad

range mode with a low energy cut off of the transmission performed by a tantalum disk between target and detector. The second one is the lens spectrometer mode. An envelope baffle system permits electron detection in a momentum band $\Delta p/p=0.12$. To cover a large energy range the magnet current is swept. In the third mode — the recoil shadow method — a longitudinal semicylindrical baffle between target and Si(Li)-detector allows spectroscopy of delayed electrons emitted from recoil nuclei in flight. Special features of this method are high transmission, and strong suppression of the prompt δ -electron background. Lifetime measurements based on the detection of conversion electrons are possible by variation of the target position. This was tested with the $^{152}\text{Sm}(^{16}\text{O}, xn)^{168-x}\text{Yb}$ compound nuclear reaction at a recoil velocity $v_r=0.01 c$, where half lives between 0.1 ns and 1 ns were determined.

Search for Superconducting Effect on the Decay of ^{99m}Tc . H. Mazaki, S. Kakiuchi, and S. Shimizu. *Zeit. f. Phys., B*, **29**, 285 (1978). — An experimental investigation of the influence of superconductivity on the decay rate of ^{99m}Tc , λ_T , has been performed by means of a differential method. The ^{99m}Tc samples containing ^{99}Tc as a carrier were prepared by electrodeposition on a copper plated tungsten wire. For production of metallic technetium the samples were reduced in pure hydrogen gas at 800~1000°C. X-ray analysis of the samples showed they were surely metallic with an hcp structure. The lattice constants observed are $a=2.741 \text{ \AA}$ and $c=4.398 \text{ \AA}$. The transition temperature was found to be $7.5 \pm 0.2 \text{ K}$. Comparison of two sources, normal (room temperature) and superconducting (4.2 K), did not show an appreciable effect of superconductivity on the decay rate of ^{99m}Tc exceeding the limit of uncertainty of our experiment: $\Delta\lambda/\lambda_T = (1.1 \pm 2.7) \times 10^{-4}$.

Mössbauer Spectroscopy of ^{57}Fe Impurities in Technetium. T. Takabatake, H. Mazaki, and T. Shinjo. *Phys. Rev. Lett.* **40**, 1051 (1978). — The Mössbauer effect of a dilute ^{57}Fe impurity in Tc was measured for the first time. The isomer shift and the quadrupole splitting at room temperature are -0.02 ± 0.01 and $-0.13 \pm 0.02 \text{ mm/s}$, respectively. Small induced magnetic fields, -4.5 ± 1 and $-7.5 \pm 1 \text{ kOe}$, were found in external magnetic fields of 30 and 45 kOe at 4.2 K. This indicates that the magnetic character of Fe impurities in Tc lies in the intermediate region between magnetic and nonmagnetic. The induced field may be attributed to local spin fluctuation.

Observation of Positron Creation in Superheavy Ion-Atom Collision Systems. H. Backe, L. Handschug, F. Hessberger, E. Kankleit, L. Richter, F. Weik, R. Willwater, H. Bokemeyer, P. Vincent, Y. Nakayama, and J. S. Greenberg. *Phys. Rev. Lett.*, **40**, 1443 (1978). — We report the first observation of positron creation in high-energy $^{208}\text{Pb}+^{208}\text{Pb}$ collisions and establish that a dominant fraction of the positron yield is from nonnuclear origins. The excess positron intensity observed over nuclear emission and its projectile energy dependence is consistent with recent predictions for pair-creation processes in the strong time-varying electric fields produced by the combined nuclear charges of the quasimolecular system formed in the collision.

Positron Production in Heavy Ion Collisions. H. Backe, E. Berdermann, H. Bokemeyer, J. S. Greenberg, L. Handschug, F. Heßberger, E. Kankeleit, P. Kienle, Ch. Kozhuharov, Y. Nakayama, L. Richter, H. Stetteier, P. Vincent, F. Weik, and R. Willwater. *Proc. Int. Conf. Nuclear Structure, Tokyo, 1977, J. Phys. Soc. Japan, 44 Suppl. 832* (1978). — Positron production in the Pb–Pb, Pb–U, and U–U colliding systems has been studied with regard to particle energy and scattering angle at the GSI facility. Techniques have been developed to determine the major background positrons from Coulomb excitation. Good agreement with theoretical predictions is obtained.

Estimation of Ultra-High Pressure by Means of the Change in Nuclear Decay Rate. H. Mazaki. *J. Phys. E, 11*, (1978). — A new method is proposed, by which an ultra-high pressure (of the order of 10^{10} Pa or more) can be estimated by observing the change in decay rate of radioactive nuclei embedded in a pressure device.

Many-Electron Effect on the K-Shell Internal Ionization Accompanying Beta Decay. T. Mukoyama and S. Shimizu. *J. Phys. G: Nucl. Phys. 4*, (1978). — The K-shell internal ionization during beta decay has been treated relativistically on the basis of the wavefunction proposed by Greenland and Irvine. The total ionization probabilities are calculated and compared with those from the hydrogenic wavefunctions. Comparison with experimental data indicates that a discrepancy still remains between theory and experiment. A possible reason for this discrepancy is discussed.

On the Energy Loss of Fast Electrons in Thin Absorbers. T. Mukoyama, and Y. Watanabe. *Phys. Letters., 64A*, 442 (1978). — The numerical constants in the Blunck — Leisegang theory for the energy-loss distribution of electrons passing through the matter have been reevaluated accurately. The obtained results give a more precise energy-loss distribution than the usual Blunck — Leisegang theory.

K-Shell Internal Ionization and Excitation in Beta-Decay: Theoretical Study. Y. Iozumi, S. Shimizu, and T. Mukoyama. *Nuovo Cimento, 41A*, 359 (1977). — The total probability of a K-shake-off process in β -decay has been reformulated by correcting the theory by Law and Campbell. By means of the improved formulation and by adding simple corrections for the K-shake-up contribution and for the correlation effect between K electron and other bound electrons, the total K hole creation probability per β -decay has been evaluated for 24 interesting nuclides. There exist distinct disagreements between our calculated values and recent experimental data; the measured probabilities are systematically larger than our calculated ones for medium- and high-Z nuclides. This clearly indicates that the theory of K shake-off, as here corrected, is not sufficient to explain the recent experimental data. This is contrary to the conclusion recently presented by many other workers that the K-shake-off plus shake-up process is the predominant mechanism of K-shell internal ionization and excitation in β -decay. It will be necessary to introduce the β -particle-electron

correlation in future theoretical treatments.

A Program for Plotting Histograms "HIST". S. Noguchi and S. Matsuki. *Bull. Inst. Chem. Res., Kyoto Univ.*, **56**, 39 (1978). — A versatile FORTRAN program called "HIST", which plots histograms in various mode on line-printer papers, has been developed. This program is not only used in the course of the analysis of bubble chamber data, but also applicable to most of the other data reduction processes in physical science.

Re-Evaluation of Stopping Powers of Be, Al, Ti, V, Fe, Co, Ni, Cu, Mo, Rh, Ag, Ta, and Au for 28 MeV Alpha Particles. R. Ishiwari, N. Shiomi, and N. Sakamoto. *Bull. Inst. Chem. Res., Kyoto Univ.*, **56**, 47 (1978). — Stopping powers of various metallic materials for 28.8 MeV alpha particles have been measured by Ishiwari *et al.*, and were reduced to the velocity of 7.0 MeV protons. However, the reduction process was too crude so that the stopping powers were re-evaluated. The present results are lower than the previous results by about 0.5%.

The ${}^9\text{Be}(d, t){}^8\text{Be}$ and ${}^9\text{Be}(d, \alpha){}^7\text{Li}$ Reaction in the Energy Range from 12.17 MeV to 14.43 MeV. S. Tanaka. *J. Phys. Soc. Japan*, **44**, 1403 (1978). — (d, t) and (d, α) reactions on ${}^9\text{Be}$ were observed simultaneously. Angular distributions of tritons and alpha particles were measured at $E_d=12.35$ MeV and at 14.06 MeV. Excitation functions were obtained from 12.17 MeV to 14.43 MeV at 85° for tritons and at 35° for alpha particles.

DWBA fit to the (d, t_0) angular distribution gave good results and the spectroscopic factor 0.29 was obtained at both deuteron energies. (d, α) reaction is considered to occur mainly passing through the compound nucleus formation. In both reactions, the cluster structure of ${}^9\text{Be}$ seems to play an important role.

Excited States of ${}^4\text{He}$ Observed in the ${}^6\text{Li}+d$ Reaction. K. Fukunaga, T. Ohsawa, N. Fujiwara, S. Tanaka, A. Okihana, and T. Yanabu. *J. Phys. Soc. Japan*, **44**, 1413 (1978). — Energy spectra of alpha particles from the ${}^6\text{Li}(d, \alpha){}^4\text{He}^*$ reaction at 13.6 MeV were observed at extremely forward angles. Angular correlations between alpha particles and deuterons were obtained for the ${}^6\text{Li}(d, \alpha d)\text{D}$ reaction when the alpha particles were detected at 20° using coincidence method. Energy spectrum of alpha particles shows a broad peak corresponding to the excited state of 25.52 MeV in ${}^4\text{He}$ with the width of 2.26 MeV. The spin-parity of this state is assigned to be 0^+ from the facts that the angular distributions of the emitted alpha particles are reproduced with DWBA theory assuming the angular momentum transfer of 2 and that the angular correlation function shows an isotropic distribution.

In the coincidence energy spectrum of alpha particles a peak corresponding to the excited state of 27.5 MeV in ${}^4\text{He}$ was observed. The angular correlation for the excited state of 27.5 MeV is consistent with the assignment of odd parity.

Differential Cross Sections of $\text{D}(d, d)\text{D}$, $\text{D}(d, p)\text{T}$, and $\text{D}(d, {}^3\text{He})n$ Reactions at 13.2 MeV. A. Okihana, N. Fujiwara, H. Nakamura-Yokota, T. Yanabu, S.

Tanaka, T. Higo, and T. Sekioka. *Proc. Int. Conf. on Nuclear Structure, Contributed Papers, Tokyo, Sept. 1977*, 7 (1977). — $d-d$ elastic scattering was measured down to 6° in the laboratory system. Analysis shows that $d-d$ potential should be repulsive. This is in accord with the fact that no Coulomb-nuclear interference was observed. The angular distributions of (d, p) and (d, n) reaction, which was derived from $(d, {}^3\text{He})$ reaction, coincided very well. No discrepancy such as reported by Brolley was found.

The ${}^3\text{He}(\tau, \tau p)d^*$ and ${}^3\text{He}(\tau, \tau d)p$ Reactions at 120 MeV and Possible Evidence for 3-N Resonances. N. Fujiwara, K. Fukunaga, T. Ohsawa, S. Tanaka, H. Nakamura-Yokota, A. Okihana, T. Sekioka, T. Higo, T. Miyayaga, and T. Yanabu. *Proc. Int. Conf. on Nuclear Structure Contributed Papers, Tokyo, Sept. 1977*, 20 (1977). — Three and four-body breakup in the ${}^3\text{He}(\tau, \tau p)d^*$ and ${}^3\text{He}(\tau, \tau d)p$ reactions were studied with 120 MeV ${}^3\text{He}$ beam from the AVF cyclotron of R.C.N.P., Osaka University. $\tau-d$ and $\tau-p$ correlation spectra show bumps except the quasi-free scattering between τ and p , and indicate possible existence of resonance state between p and d or d^* .

Elastic and Inelastic Scattering of ${}^3\text{He}$ by ${}^3\text{He}$ at 120 MeV. S. Tanaka, T. Ohsawa, K. Fukunaga, N. Fujiwara, H. Nakamura-Yokota, A. Okihana, T. Sekioka, T. Higo, T. Miyayaga, and T. Yanabu. *Proc. Int. Conf. on Nuclear Structure, Contributed Papers, Sept. Tokyo, 1977*, 21 (1977). — Elastic and inelastic scattering of ${}^3\text{He}$ off ${}^3\text{He}$ were studied at 120 MeV. The observation was made down to 7° in the laboratory system and statistical errors were less than 2%. Elastic scattering can be fitted by an optical model potential but parameters deviate strongly from those of commonly accepted values. Energy spectra of inelastic ${}^3\text{He}$ show bumps at forward angles, and these bumps are possibly due to the final state interaction between p and d or p and d^* .

${}^{11}\text{B}(p, 2\alpha)\alpha$ Reaction and Three Alpha Resonance of ${}^{12}\text{C}^*$. T. Ohsawa, K. Fukunaga, T. Sekioka, N. Fujiwara, S. Tanaka, A. Okihana, T. Higo, and S. Kakigi. *Proc. Int. Conf. on Nuclear Structure, Contributed Papers, Sept. Tokyo, 1977*, 165 (1977). — Broad resonance-like peak was observed in the ${}^{11}\text{B}(p, \alpha_1){}^8\text{Be}(1\text{st})$ reaction at around $E_p=7.27$ MeV. Correlation functions between α_1 and α_2 particles from the ${}^{11}\text{B}(p, \alpha_1){}^8\text{Be}(1\text{st}) (\alpha_2){}^4\text{He}$ reaction were measured at $E_p=7.27$ MeV (on resonance) and 6.67 MeV (off resonance). Analysis shows that there exists a resonance state of ${}^{12}\text{C}^*(3^-)$ at the excitation energy of 22.7 MeV, and this state has a large component of the ${}^8\text{Be}(2^+)-\alpha$ structure.

Material Analysis by the Nuclear Backscattering Method Using Cyclotron. Y. Hayashi, T. Igaki, and H. Takekoshi. *Bull. Inst. Chem. Res., Kyoto Univ.*, **56**, 11 (1978). — Organic matters have been analyzed with nuclear backscattering method using the Kyoto University cyclotron. The energies of the beams used in these experiments are higher than those commonly used in the nuclear backscattering analysis. About the local distribution of light elements in the samples, the resolution

of about 1 micron at the depth of 20 micron is obtained. The elemental ratio can be decided precisely for the sample of 5×10^{16} molecules/cm².

Energy Straggling of 6.74 MeV Protons in Cu. N. Sakamoto, N. Shiomi, R. Ishiwari, and J. Miyajima. *Bull. Inst. Chem. Res., Kyoto Univ.*, **56**, 20 (1978). — Energy straggling of 6.74 MeV protons in Cu foils has been measured. Foils are commercially prepared and approximately 3.9 mg/cm² thick. Measurements have been made for two different thicknesses, using one foil and two foils. The straggling results are compared with theoretical predictions of Vavilov. The energy straggling greater than theoretical predictions is considered to be the effect of foil non-uniformity. It has been shown that the energy loss measurement with non-uniform target gives the same results as the measurement with uniform target, supposing the mean thickness of non-uniform target is equal to the thickness of uniform one.

Analytical Chemistry

Extraction Behavior of Metal Benzoyltrifluoroacetates. T. Honjo, M. Matsui, and T. Shigematsu. *Bull. Inst. Chem. Res., Kyoto Univ.*, **55**, 415 (1977). — The behavior of trace amounts of iron, cobalt, copper, zinc, indium, uranium, zirconium, scandium, lanthanum, cerium, neodymium, samarium, europium, terbium, ytterbium, and lutetium in solvent extraction has been reviewed in order to ascertain the basic conditions for the separation of metals as their benzoyltrifluoroacetates by solvent extraction. The pH of the half extraction decreases in the following order: Co(II)–Zn(II)–La(III)–Nd(III)–Ce(III)–Eu(III)–Tb(III)–Sm(III)–Yb(III)–Lu(III)–In(III)–UO₂(II)–Fe(III)–Sc(III)–Cu(II)–Zr(IV). The extraction constants for the benzoyltrifluoroacetate chelates tend to increase with an increase in the ionic potential of the metals. The variation of the extraction constants of rare earth chelates with atomic number of rare earth elements shows interesting tetrad effects.

Some Aspects of the Tetrad Effect in the Synergic Extraction of Rare Earth β -Diketonate Adducts with *n*-Hexyl Alcohol, TBP, and TOPO. T. Honjo, M. Matsui, and T. Shigematsu. *Bull. Inst. Chem. Res., Kyoto Univ.*, **55**, 423 (1977). — The extraction constants of rare earth chelates, $-\log K$, and the overall stability constants of their adducts, $\log \beta$, were determined by the solvent extraction of rare earth elements such as lanthanum(III), cerium(III), neodymium(III), samarium(III), europium(III), terbium(III), ytterbium(III), and lutetium(III) with BFA (benzoyltrifluoroacetone) with or without *n*-hexyl alcohol, TBP (tri-*n*-butyl phosphate) and TOPO (tri-*n*-octylphosphine oxide) in benzene. The variation of $-\log K$ and $\log \beta$ with atomic number of rare earth elements, *Z*, was found to show interesting tetrad effects. Abnormal behavior of trace amounts of cerium(III) during the extraction was investigated by using various β -diketones such as AA (acetylacetone), BzA (benzoylacetone), TFA (trifluoroacetylacetone), and BFA with or without TOPO in benzene. The apparent changes of free energy, enthalpy, and entropy in the extraction of lutetium(III) with DPM (dipropionylmethane), BzA with or without TOPO in benzene were also estimated to get true information on the

mechanism of the synergic extraction.

Spectrophotometric Determination of Chromium(III) and Chromium (VI) in Sea Water. T. Shigematsu, S. Gohda, H. Tamazaki, and Y. Nishikawa. *Bull. Inst. Chem. Res., Kyoto Univ.*, **55**, 429 (1977). — Fundamental conditions for the state analysis of chromium in sea, lake, and river water were studied, and procedures for the particle fractionation and the separation of chromium(III) from chromium(VI) were recommended.

Some sea, lake, and river water samples were analyzed, and 0.01–0.27 $\mu\text{g Cr(III)/l}$ and 0.04–0.47 $\mu\text{g Cr(VI)/l}$ were obtained. In open sea chromium(VI) was predominant.

Electron Paramagnetic Resonance Studies of Cobalt(II) Thioiminato Schiff Base Compound with Lewis Bases and Its Oxygen Adducts. M. Sakurada, Y. Sasaki, M. Matsui, and T. Shigematsu. *Bull. Inst. Chem. Res., Kyoto Univ.*, **55**, 466 (1977). — EPR spectra were observed for *N, N'*-ethylenebismonothioacetylacetoniminatocobalt(II), $\text{Co(sacac)}_2\text{en}$, with the Lewis bases, LB, (pyridine, 4-methylpyridine, 4-cyanopyridine, piperidine, *N*-methylimidazole and *N, N*-dimethylformamide) and their oxygen complexes. The EPR spectra show that all of the $\text{Co(sacac)}_2\text{en(LB)}$ complexes have the rhombic symmetry with $(d_{x^2-y^2}, d_{zz}, d_{yz})^6(d_{z^2})^1$ ground configuration. Cobalt-59 hyperfine coupling constants are utilized in evaluating the unpaired electron spin distribution. The total cobalt spin densities are found to fall in the range of 0.66–0.78 and to be mainly localized on the cobalt atom for $\text{Co(sacac)}_2\text{en(LB)}$. $\text{Co(sacac)}_2\text{en(Lb)}$ forms a monomeric 1:1 complex with molecular oxygen reversibly. It is found that the EPR parameters of the oxygen adducts are very similar for these Lewis bases.

The Standard Reference Materials and the Precision of Analytical Values in Environmental Analysis. T. Kiba, H. Akaiwa, M. Ichikuni, T. Ozawa, M. Kamada, Y. Kitano, T. Shigematsu, N. Suzuki, T. Sotobayashi, K. Nagashima, Y. Nishikawa, M. Nishimura, H. Hamaguchi, T. Matsuo, Y. Murakami, M. Murozumi, Y. Morita, N. Yamagata, Y. Yamamoto, and K. Watanuki. *Bunseki Kagaku (Japan Analyst)*, **26**, T12 (1977), in Japanese. — During the last two years 1975~1976 a research group was organized to evaluate jointly the precision of trace analysis values for environmental samples. The twenty-membered group, supported by a Grant-in-aid for Scientific Research from the Ministry of Education (No. 011010), cooperated in the interlaboratory comparison tests of two reference standard materials, *i.e.* a natural water sample and a composite heavy metal salts solution. The natural water sample was collected at Watarase River on November 11, 1975. The river water and the salts solution were distributed among the members and analyzed, respectively, for Cu, Zn, and Pb and for Cu, Zn, Cd, Pb, Cr, and Fe. Results are listed in Tables 1 and 3. In these trials all members were free of a specified pre-treatment and of a defined measurement technique, and therefore the results obtained seem to give the average precision of the analyses carried out arbitrarily in the university laboratories: the coefficients of variation fall in ten percent order for metals in lower concentration

as in river water, and in only a few percent for the same metals in higher concentration and in their stable forms as in the synthesized sample solution.

The Fluorescence Properties of Metal Complexes of Salicylaldehyde-semicarbazones and Their Use in Fluorometry; Fluorometric Determination of Aluminum in Sea Water. K. Morisige, K. Hiraki, Y. Nishikawa, and T. Shigematsu. *Bunseki Kagaku (Japan Analyst)*, **27**, 109 (1978), in Japanese. — Eleven Schiff bases, which are derived from salicylaldehyde-semicarbazone, were synthesized, and the effect of the position of substituent groups on the fluorescence properties of metal complexes was studied. The compounds of these types formed the fluorescent complexes with aluminum, gallium, scandium, yttrium, and zinc ions. In generally, substitution by *o*, *p*-orientating substituents at *p*-position to $-\text{CH}=\text{N}-$ group of Schiff bases and substitution by *m*-orientating substituents at *m*-position increased fluorescence sensitivity index (F.S.I.) and molar extinction coefficient of the complexes. These values correlated with Hammett's substituent constant. The phenomenon may be explained by the concept of charged quinoid form, and significant contribution of charged quinoid form enhanced the fluorescence ability of the complexes. 2, 4-Dihydroxybenzaldehyde-semicarbazone proved a good fluorescence reagent for aluminum determination, on account of the stability and sensitivity of fluorescence, and then, this reagent was used for the rapid and accurate determination of aluminum in sea water.

Report of the Co-operative Research (Preservation of Marine Environment) Minist. Educ. Sci. Cul. T. Shigematsu, M. Nishimura, and M. Murozumi. *Showa Goju-ichi nendo Monbusho Kagaku Kenkyu ni yoru Tokutei Kenkyu no Chukan Hokokusho I*, "Kaiyo Kankyo Hozen no Kisotekikenkyu" (*Chem. Anal. of Inorg. micro-constituents in sea water*), 169 (1977), in Japanese. — Review.

Physical Chemistry

Systematic Analysis to Determine the Dielectric Phase Parameters from Dielectric Relaxations Caused by Diphasic Structure of Disperse Systems. T. Hanai, A. Ishikawa, and N. Koizumi. *Bull. Inst. Chem. Res., Kyoto Univ.*, **55**, 376 (1977). — A systematic method is proposed to estimate the relative permittivity, the electrical conductivity and the volume fraction of the disperse phase from dielectric relaxation due to diphasic structure in spherical disperse systems. On the basis of Wagner's and Hanai's theory of interfacial polarization, theoretical expressions of practical use are derived for i) a system with non-conducting disperse phase, ii) a system with non-conducting continuous phase, and iii) a general system. Since the relations derived for the general case are of a complicated nature on evaluating the roots, some remarks are given to perform computer-searching for numerical solutions of the equations. The relations derived were applied to dielectric data of an oil-in-water emulsion, a water-in-oil emulsion, and a suspension of Sephadex G-25 in water to estimate the permittivity, the conductivity and the concentration of the disperse phase for the respective systems. For the disperse systems considered, the dielectric

relaxation profiles were represented satisfactorily by Hanai's theory.

Dielectric Properties of Protoplasm, Plasma Membrane and Cell Wall in Yeast Cells. K. Asami. *Bull. Inst. Chem. Res., Kyoto Univ.*, **55**, 394 (1977). — Dielectric behavior of yeast cell suspensions has been studied to elucidate dielectric properties of protoplasm, plasma membrane and cell wall. Conductivity of the cell wall showed the behavior similar to that of an ion-exchange resin membrane owing to ionized compounds in the cell wall. The concentration of the ionized compounds was estimated to be 0.011 equiv/l. Since the cell wall had the same conductivity as that of the suspending medium with KCl concentrations ranging from 10 mM to 80 mM, an electrical model of single-shell spheres may substantially be applied to the yeast cells. An analysis of the dielectric data was carried out by use of Pauly and Schwan's theory. The membrane capacitance was estimated to be $1.1 \mu\text{F}/\text{cm}^2$ and was unaffected by changes in salt concentration and osmolarity of the suspending medium. No change in the conductivity of the protoplasm was observed with variation of KCl concentration of the outer medium. This suggests that the salt concentration in the aqueous phase of the protoplasm is kept unchanged irrespective of the KCl concentration of the outer medium. The conductivity and the dielectric constant of the protoplasm was lower in comparison to the outer electrolyte solution. This may be attributed to the presence of intracellular organelles and proteins. The osmotic behavior of the yeast cells was also studied by dielectric technique. Plasmolysis was found to occur in suspending mediums with osmolarities higher than 1 osM.

Artificial Membranes. T. Hanai. *Seikagakuzik'kenkoza Vol. 14, "Biomembranes"* pp. 261–271, edited by the Biochemical Society of Japan, Tokyo-Kagakudozin, (1977), in Japanese. — Techniques are described for biochemists to review the experiments of artificial membranes such as underwater bimolecular lipid membranes and built-up films composed of monolayers at an air-water interface.

Passive Electrical Properties of Cultured Murine Lymphoblast(L5178Y) with Reference to Its Cytoplasmic Membrane, Nuclear Envelope, and Intracellular Phases. A. Irimajiri, Y. Doida, T. Hanai, and A. Inouye. *J. Membrane Biol.*, **38**, 209 (1978). — Dielectric dispersion measurements over a frequency range 0.01–100 MHz were made with the suspensions of a cultured cell line, mouse lymphoma L5178Y, and an attempt to explain the observed dielectric behavior by taking explicitly into consideration the possible involvement of cell nucleus has been presented.

The use of a conventional "single-shell" model in which the cell is represented by a homogeneous sphere coated with a thin limiting shell phase did not duplicate the observed dispersion curves, whereas a "double-shell" model in which one additional concentric shell is incorporated into the "single-shell" model gave a much better fit between the observed and the predicted dispersion curves. Based on the latter model, we analyzed the raw data of dielectric measurements to yield a set of plausible electrical parameters for the lymphoma cell: $C_M \simeq 1.0 \mu\text{F}/\text{cm}^2$, $C_N \simeq 0.4 \mu\text{F}/\text{cm}^2$, $\epsilon_K \simeq 300$, $\kappa_c/\kappa_a \simeq 0.9$, and $\kappa_k/\kappa_c \simeq 0.7$. Here, C_M and C_N are the specific capacities of plasma and nuclear membranes; ϵ and κ are the dielectric constant and conductivity with sub-

script a , c , and k referring respectively to the extracellular, the cytoplasmic and the karyoplasmic phases.

Bimolecular Lipid Membranes. T. Hanai. *Shin-Zikkenkagaku Koza Vol. 18*, "Interfaces and Colloids", pp. 476-497, edited by the Chemical Society of Japan, Maruzen, (1977), in *Japanese*. — This treatise, which is Chapter 6 in a volume entitled "Interfaces and Colloids", is a detailed description of practical techniques for carrying out the experiments of underwater black lipid membranes (BLM). The contents are the followings: 1) Lipids to form the BLM. 2) Apparatus for BLM formation. 3) Preparation of the BLM forming solutions. 4) Practice of BLM formation. 5) Measurements of areas, electric resistances and capacitances of the BLM. 6) Techniques of BLM formation by means of the apposition of two lipid monolayers at an air-water interface.

Dielectric Behavior of Vinylidene Fluoride-Hexafluoropropylene Copolymers. N. Koizumi, M. Kuzuhara, and S. Koizumi. *ACS Organic Coatings and Plastics Chemistry*, **38**, 340 (1978). — Dielectric behavior of vinylidene fluoride (VDF) — hexafluoropropylene (HFP) copolymers with HFP contents of 5 to 37.4 mol-% has been investigated over a wide range of frequency at temperatures between 170 and 320 K. Most of copolymers studied were amorphous, the one with 5 mol-% HFP being partially crystalline. The glass transition temperature increased from 233 to 270 K with increasing HFP contents. Copolymers exhibited three relaxation processes α , β , and γ , in decreasing order of temperature. The α relaxation found only for the copolymer with 5 mol-% HFP was attributed to molecular motions in crystalline regions. The β and γ relaxations appeared above and below the glass transition respectively. The former was assigned to the micro-Brownian motions of backbone molecular chains; the latter to the local mode relaxation of short VDF sequences. The dielectric loss as a function of frequency revealed that the relaxation consisted of two closely situated loss peaks, β_1 and β_2 , at low and high frequency, respectively. The magnitude of the β_1 relaxation increased at low temperature, particularly for copolymers with higher HFP contents. The β_1 process was interpreted in terms of cooperative rearrangements of long molecular chains containing HFP units. The higher the temperature, the greater was the magnitude of the β_2 relaxation. This implies that relaxation is associated with motions of segments composed of the VDF sequence and the number of such segments taking part in the molecular orientation increases at high temperatures.

Oriented Adsorption of Tetrahalogenoethylene on Alkali Halide. H. Saijo. *Bull. Inst. Chem. Res., Kyoto Univ.*, **55**, 355 (1977). — Adsorption states of tetrahalogenoethylene (TXE) on KCl(100) cleaved surface were studied by means of LEED and AES in relation to the previous work for tetracyanoethylene. After the adsorption, LEED patterns did not give any indication of superlattice formation, although variations of the diffraction intensities were observed. The remarkable decrease of Auger intensity from potassium on adsorption was discussed comparing the sizes of halogen atoms in the adsorbed molecules. It was deduced that four halogen

atoms of each TXE molecule sat right on the potassium ions of the substrate surface, while C=C group settled on the chlorine ion with random orientation. A simple and easy method to detect the change of surface states is proposed.

A New Theoretical and Practical Approach to the Multislice Method.

K. Ishizuka and N. Uyeda. *Acta Cryst.* **A33**, 740 (1977). — The multislice formulation of Cowley and Moodie for high-energy electron scattering is rederived from the Schrödinger equation; and the validity of the finite slice approach in practical computation is theoretically proved by the stationary-phase approximation. A set of computer programs for the multislice method is developed, where the convolution integral is carried out through the fast Fourier transform. The following conditions are required to obtain a sufficiently accurate result in multislice calculations: (1) the maximum slice thickness should be about kd^2 , where k is the wavenumber of the incident electrons and d is the distance over which the potential does not change appreciably; (2) there must be a sufficient number of beams in the multislice iteration to prevent the aliasing effect of convolution. The multiple scattering masks the real specimen structure when the specimen thickness exceeds a certain value. This effect of multiple scattering is recognized from the probability distribution of the scattered electrons in addition to the scattering amplitudes obtained through the procedure developed in the present work.

Epitaxial Growth of a New Polymorph of Cu-Phthalocyanine on Graphite.

H. Saijo, T. Kobayashi, and N. Uyeda. *J. Crystal Growth*, **40**, 118 (1977). — The epitaxial growth of Cu-phthalocyanine vacuum deposited on cleaved surfaces of graphite was studied by means of electron microscopy and selected area electron diffraction. The analysis of tilted diffraction patterns revealed that the epitaxial crystallite of Cu-phthalocyanine assumes a new polymorph with an orthorhombic unit cell whose dimensions are $a=14.9$, $b=12.2$, and $c=13.7$ Å. Epitaxial crystallites of Cu-phthalocyanine were found to assume a high-index plane such as $(2\bar{5}3)$, at the interface. The appearance of the crystallites and the formation of the new polymorph were ascribed to the strong π -electronic interaction at the surface. This interaction is thought to control the oriented adsorption of the molecule upon the surface lattice of the graphite substrate, resulting in formation of epitaxial nuclei of the new polymorph.

The Measurement of Interaction Force on Microparticles.

M. Arakawa and S. Yasuda. *Zairyo (J. Soc. Mater. Sci., Japan)*, **26**, 858 (1977) in Japanese. — The interaction force between microparticles was measured with an electrobalance directly in various atmospheric conditions, particularly in the humidity controlled air, nitrogen, and vacuum. The interaction force of glass microspheres in a dried atmosphere changed inversely as the square of the distance between two particles. It was considered that the attractive force was resulted from the Coulomb force between the particles.

The interaction force between the hydrophilic particles in humid air was so little as to be neglected when the particles were brought close together. But the cohesive

force of the particles needed to separate them each other was larger than the Coulomb force and it varied with humidity of air. The cohesive force did not change at the lower humidity range, but increased rapidly at the humidity of 60% R.H. or above. These results suggest that in a humid atmosphere the interaction force between the particles results from the capillary condensation of water vapor associated with the contact of two particles.

Electron Wave Optical Identification of Specific Atoms in Thin Crystals. N. Uyeda, T. Kobayashi, Y. Fujiyoshi, and K. Ishizuka. *Thirty-Fifth Annual EMSA Meeting*, 30 (1977). — Review.

Solid-Liquid Adhesion of Oxidized Polyethylene Films. Effect of Temperature on Polar Forces. A. Baszkin, M. Nishino, and L. Ter-Minassin-Saraga. *J. Colloid and Interface Sci.*, **59**, 516 (1977). — The nonpolar polyethylene is transformed by oxidation into a superficially polar polyethylene with a known surface density of carbonyl groups. The dispersion and polar contributions to the free energy of adhesion for the systems oxidized and unoxidized polyethylene with *n*-octane, water and methylene iodide are calculated. The variation of γ_s^d , γ_s^p and γ_{s1} with temperature is found to verify the geometric mean equation for the interfacial free energy $\gamma_{s1} = \gamma_s + \gamma_1 - 2(\gamma_s^d \gamma_1^d)^{1/2} - 2(\gamma_s^p \gamma_1^p)^{1/2}$. The results are analyzed and the importance of the dispersion and polar interactions and their dependence on temperature is discussed.

Atomic Resolution with Image Processing of High Voltage Electron Micrographs. B. Siegel, N. Uyeda, and E. Kirkland. *Proc. Fifth Int. Conf. on High Voltage Electron Microscopy, Kyoto, 1977*, 289 (1977). — Review.

Vibrational Spectra of 1, 2, 4, 5-Tetracyanobenzene and 1, 2, 4, 5-Tetracyanobenzene- d_2 Crystals. T. Takenaka, J. Umemura, S. Tadokoro, S. Oka, and T. Kobayashi. *Bull. Inst. Chem. Res., Kyoto Univ.*, **56**, 176 (1978). — Polarized IR and far-IR spectra of single crystals of 1, 2, 4, 5-tetracyanobenzene and 1, 2, 4, 5-tetracyanobenzene- d_2 were recorded. Polarized Raman spectra of these samples were also obtained at various geometries of the sample excitation and polarization. The results were analyzed under the assumption of the oriented gas model. The assignment of the fundamental frequencies was made with the aid of the isotope frequency shift and the spectral data of related compounds. The normal coordinate calculations were carried out with the modified Urey-Bradley force field and the valence force field for the in-plane and out-of-plane vibrations, respectively.

Vibrational Spectra of Tetracyano-1, 4-dithiin. J. Nakanishi and T. Takenaka. *Bull. Inst. Chem. Res., Kyoto Univ.*, **56**, 192 (1978). — Infrared spectra of the tetracyano-1, 4-dithiin (TCND) crystal were recorded at the normal incidence of polarized radiation upon the (010) sample plane at various angles between the electric vector of the incident radiation and the *a* crystal axis from 0° to 180°. Polarized Raman spectra of the crystal were also recorded. The depolarization ratios of the Raman bands were obtained in solutions. From the results obtained, the infrared

and Raman bands were classified into four symmetry species of the C_{2v} molecular group under the assumption of the oriented gas model. Assignments of the observed bands to the individual fundamental vibrations were carried out with the aid of the above-mentioned examinations, the spectral data of analogous molecules, and the normal coordinate analysis.

Sensitive Measurements of Photodichroism of Anthracene by Spectropolarimeter. N. Kimura and S. Hayashi. *Bull. Inst. Chem. Res., Kyoto Univ.*, **56**, 213 (1978). — Anthracene molecules dispersed in polyvinylchloride (PVC) films were irradiated by polarized light of wavelength 257 or 383 nm. The induced photodichroism (Weigert effect) was recorded sensitively by means of a spectropolarimeter. The sample irradiated by polarized light of 257 nm shows perpendicular dichroism at 257 nm and parallel dichroism at 383 nm. While, the sample irradiated by polarized light of 383 nm shows parallel dichroism at 257 nm and perpendicular dichroism at 383 nm. The several bands in the region of 300–400 nm were analyzed as superposition of absorptions polarized to the short axis direction of the anthracene molecule upon those polarized to the long axis direction of the molecule.

Effect of Electrolyte on the Molecular Orientation in Monolayers Adsorbed at the Liquid-Liquid Interface: Studies by Resonance Raman Spectra. T. Takenaka. *Chem. Phys. Letters*, **55**, 515 (1978). — Polarization measurements of resonance Raman spectra were made for monolayers of a surface-active azo dye adsorbed at the interface between carbon tetrachloride and an aqueous solution and an effect of electrolyte on the molecular orientation in the monolayers was examined.

Polarized Raman Spectra of Lanthanum Ethylsulfate Nonahydrate and Potassium Ethylsulfate Crystals. Y. Kato, T. Kurimoto, and T. Takenaka. *Spectrochim. Acta*, **33A**, 1033 (1977). — The polarized Raman spectra of $\text{La}(\text{C}_2\text{H}_5\text{SO}_4)_3 \cdot 9\text{H}_2\text{O}$, $\text{La}(\text{C}_2\text{H}_6\text{SO}_4)_3 \cdot 9\text{D}_2\text{O}$ and $\text{KC}_2\text{H}_5\text{SO}_4$ crystals have been observed from 30 to 4000 cm^{-1} at room temperature. The observed bands have experimentally been classified into each Raman-active symmetry species. From the far-infrared spectra from 30 to 300 cm^{-1} of $\text{La}(\text{C}_2\text{H}_5\text{SO}_4)_3 \cdot 9\text{H}_2\text{O}$, the absorption bands of the infrared-active E_{1u} species have also been obtained. The vibrational assignment for the ethylsulfate group has been made by comparing the spectra of $\text{La}(\text{C}_2\text{H}_5\text{SO}_4)_3 \cdot 9\text{H}_2\text{O}$ and $\text{La}(\text{C}_2\text{H}_5\text{SO}_4)_3 \cdot 9\text{D}_2\text{O}$ with those of $\text{KC}_2\text{H}_5\text{SO}_4$ and using a group-theoretical consideration.

Change of Molecular Configuration in Crystalline Decanoic Acid as Studied by Infrared Spectra and Normal Coordinate Analysis. J. Umemura. *J. Chem. Phys.*, **68**, 42 (1978). — Infrared spectra of a well-oriented crystalline film of decanoic acid were obtained in the range from room temperature to liquid-helium temperature. Many absorption bands due to the carboxyl group and a band progression due to the CH_2 wagging modes appear as doublets. In each doublet, one component decreases in intensity with lowering temperature and disappears near liquid-helium temperature (type I), while another component increases in intensity

with lowering temperature (type II). It is confirmed by normal coordinate analysis that the type I and II bands are ascribed to fundamental vibrations of the *cis* and *trans* isomers, respectively. The latter isomer would be produced from the former by double proton transfer in the decanoic acid dimer. From the temperature dependence of band intensities, the enthalpy and entropy differences between the two isomers are evaluated to be about 240 cal·mol⁻¹ and 3.8 cal·mol⁻¹·deg⁻¹, respectively.

The Effect of Double Layer Interaction on the Drainage of Thin Liquid Films. M. Matsumoto, C. Montandon, S. Hartland, and A. Watanabe. *Chem. Engineering Sci.*, **33**, 831 (1978). — The drainage of thin liquid films of an aqueous solution containing anionic surfactant and inorganic electrolyte between platinum and a mercury pool electrode was examined by the capacitance method. The system consisted of either symmetrical or unsymmetrical potentials of diffuse double layers which were estimated by differential capacitance measurements. The results showed that the drainage of the liquid film initially took place quickly and then slowly attained an equilibrium thickness. This general tendency could be explained qualitatively by the theoretically calculated disjoining pressure but the equilibrium thickness of 7–13 nm was too small to be explained in terms of electrostatic repulsion and van der Waals attraction. Hence, it was supposed that other forces, such as steric hindrance, are acting to thicken the film in addition to the above mentioned disjoining pressure. The force acting on the film obtained from the Reynolds equation also indicates the presence of other forces which are acting to thin the film in addition to gravity.

Synthesis of Dimethyl Formamide from Carbon Dioxide, Hydrogen and Dimethyl Amine Catalyzed by Palladium(II) Chloride. K. Kudo, H. Phala, N. Sugita, and Y. Takezaki. *Chemistry Letters*, 1495 (1977). — Dimethyl formamide was catalytically synthesized from dimethyl amine, carbon dioxide and hydrogen in the presence of palladium(II) chloride and bases in the methyl cellosolve.

Studies on the High Pressure Reactions Utilizing CO and CO₂. (Prize Address, Review). Y. Takezaki. *J. Japan Petrol. Inst.*, **20**, 655 (1977) in Japanese. — Developments on the above-titled investigations made in our laboratory during these 20 years have been reviewed, stress being laid on the kinetics and mechanism of the reactions. Used Catalysis were acids in broad sense, bases, and some noble metals and their complexes, while the substrates were alcohols, ketones, olefins and unsaturates with functional groups, saturated halides, aromatics, amines, organic acid salts, etc.

Mechanism of Carbon Monoxide Reactions under High Pressure Catalyzed by Acids or Bases. Y. Takezaki. *J. Japan Petrol. Inst.*, **21**, 143 (1978). — Review: The reactions of carbon monoxide under high pressure have been reviewed to show the results of some representative examples of kinetic and mechanism investigations performed in our laboratory.

In the acid catalyzed reactions, three distinct patterns have been obtained, *viz.*, the formation of carbonium cation by protonation with protonic acid, the intermediate

formation of sultone-like structure by SO_3 , and the ion pair production of protonated cation with Lewis acid, all prior to CO addition.

In the base catalyzed reactions, two kinds of patterns have been recognized so far, *viz.* the substrate and the base produce an active species which then reacts with CO, and the base combines with CO to form an active complex initially which then attacks the substrate.

Inorganic Chemistry

Formation of Metastable δ -Form of $6\text{Bi}_2\text{O}_3 \cdot \text{SiO}_2$ Crystal from Its Melt.

S. Ito, T. Kokubo, and M. Tashiro. *Bull. Inst. Chem. Res., Kyoto Univ.*, **55**, 447 (1977). Levin *et al.* reported that the γ -form of $6\text{Bi}_2\text{O}_3 \cdot \text{SiO}_2$ has an equilibrium melting temperature of 900°C , being most stable at least down to 600°C . The present authors, however, have found that the γ -form never precipitates from a thoroughly homogenized melt of the same composition even when the melt is cooled slowly, *e.g.* at a rate as low as $0.2^\circ\text{C}/\text{min}$: The melt is supercooled down to 740°C , where a metastable δ -form of $6\text{Bi}_2\text{O}_3 \cdot \text{SiO}_2$ precipitates in the supercooled melt in place of the γ -form.

The high energy barrier for formation of the γ -form as well as the low energy barrier for formation of the δ -form were explained in terms of similarity in microstructure of the γ - and δ -form with their melt: The δ -form has a more open, defective and symmetric structure which is similar to that of the melt than that of the γ -form. Stability relationships of the γ - and δ -form with their melt were determined in detail.

Transformation of Metastable δ -Form of $6\text{Bi}_2\text{O}_3 \cdot \text{SiO}_2$ and Its Melt into Stable γ -Form Induced by Mechanical Tapping.

S. Ito, T. Kokubo, and M. Tashiro. *Bull. Inst. Chem. Res., Kyoto Univ.*, **55**, 457 (1977). — The supercooled $6\text{Bi}_2\text{O}_3 \cdot \text{SiO}_2$ melt precipitated spontaneously only metastable δ - $6\text{Bi}_2\text{O}_3 \cdot \text{SiO}_2$ crystals when cooled still in a Pt-crucible without giving any mechanical shock, while it precipitated stable γ - $6\text{Bi}_2\text{O}_3 \cdot \text{SiO}_2$ crystals when the Pt-crucible was intensively tapped with a hard rod such as an alumina rod in the course of cooling. The δ -crystals once precipitated spontaneously from the melt never transformed into the γ -crystals on further cooling when cooled still, while they transformed into the γ -crystals when the crucible was intensively tapped in the course of cooling. The precipitation of the γ -crystals from the melt induced by the tapping was attributed to formation of cavities in the melt, and the transformation of the δ -crystals into the γ -crystals induced by the tapping was attributed to formation of dislocations in the δ -crystals; both the cavities in the supercooled melt and dislocations in the δ -crystals were thought to accelerate nucleation of the γ -crystals.

Transparency of LiTaO_3 - SiO_2 - Al_2O_3 Glass-ceramics in Relation to Their

Microstructure. S. Ito, T. Kokubo, and M. Tashiro. *J. Materials Sci.*, **13**, 930 (1978). — The glasses with various compositions in the LiTaO_3 - SiO_2 - Al_2O_3 system were heated from room temperature to temperatures ranging from 750°C to 1050°C at a rate of $5^\circ\text{C}/\text{min}^{-1}$. From the glasses in the LiTaO_3 - SiO_2 system no transparent glass-ceramic was obtained even when their $\text{LiTaO}_3/\text{SiO}_2$ mole ratios were as high as

2.33. The diameter and number of the LiTaO_3 crystal grains precipitated in the glass were 5–15 μm and 10^8 – 10^{10} grains/ cm^{-3} , respectively. On the contrary, transparent glass-ceramics were obtained from the glasses containing Al_2O_3 ; their compositions covered a fairly large area in the LiTaO_3 – SiO_2 – Al_2O_3 system, which encompasses the compositions with the $\text{LiTaO}_3/\text{SiO}_2 + \text{AlO}_{1.5}$ mole ratio as low as 0.25. The diameter and number of the LiTaO_3 crystal grains precipitated in the transparent glass-ceramics were as small as 10–20 nm and as many as 10^{16} – 10^{18} grains/ cm^{-3} , respectively. High nucleation rates of the LiTaO_3 crystals in the Al_2O_3 -containing glasses were interpreted in terms of structural inflexibility induced in the glass-network by the addition of Al_2O_3 to the LiTaO_3 – SiO_2 system.

Prick-Induced Crystallization of Supercooled $6\text{Bi}_2\text{O}_3 \cdot \text{SiO}_2$ Melt. M. Tashiro, T. Kokubo, and S. Ito. *Proceedings of XIth International Congress on Glass, II*, 167 (1977). — When a melt (about 3 g) of the composition, $6\text{Bi}_2\text{O}_3 \cdot \text{SiO}_2$, is cooled at a rate of 5–150°C/min, it is supercooled to about 740°C without transforming into the stable γ - $6\text{Bi}_2\text{O}_3 \cdot \text{SiO}_2$ crystal at its melting temperature (900°C), and at about 740°C it transforms spontaneously into metastable δ - $6\text{Bi}_2\text{O}_3 \cdot \text{SiO}_2$ crystals with a melting temperature of 750°C, which remain in the metastable state down to room temperature.

When the surface of the supercooled melt or metastable δ -crystals is pricked with the tip of a thin platinum wire during the above cooling process at temperatures above 550°C, the γ -crystal starts to form from the pricked point and spread radially and rapidly through the bulk of the melt or δ -crystals.

The rate of spontaneous growth of the δ -crystals in the melt and the rate of the prick-induced growth of the γ -crystals in the melt are 0.86 and 22 cm/min, respectively. The heat of fusion of the δ -crystal is 1/5 of that of the γ -crystal. From these data it is concluded that the kinetic energy barriers for nucleation of the γ -crystal in both the melt and δ -crystals are very high and the pricking of the surface of the melt or δ -crystals supplies sufficient energy to overcome these barriers.

Fabrication of Oriented Polycrystalline $\text{Li}_2\text{O} \cdot 2\text{SiO}_2$ Ceramic by Unidirectional Solidification of Its Melt. M. Arioka, T. Kokubo, and M. Tashiro. *Yogyo-Kyokai-Shi (Journal of the Ceramic Association, Japan)*, **85**, 501 (1977), in Japanese. — A congruently melting $\text{Li}_2\text{O} \cdot 2\text{SiO}_2$ melt was poured into a clay crucible, the inner bottom surface of which had previously been covered with a $\text{Li}_2\text{O} \cdot 2\text{SiO}_2$ glass-ceramic layer. The melt was then solidified unidirectionally from the bottom of the crucible at a rate of 3.3 mm/h. The temperature gradient in the melt was 80°C/cm. The glass-ceramic layer acted as seed crystals and a large number of $\text{Li}_2\text{O} \cdot 2\text{SiO}_2$ columnar crystals grew from the seeds with their c -axis parallel to their growth direction. The average diameter (D) of the columnar crystals decreased from 580 to 340 μm as the solidification rate (R) was increased from 0.7 to 13 mm/h, which yielded the relation, $D \propto R^{-1/6}$.

On the Existence of Intercalation Compound of Boron Nitride with Ferric Chloride. K. Ohhashi and T. Shinjo. *Bull. Inst. Chem. Res., Kyoto Univ.*, **55**, 441

(1977). — Mössbauer effect and X-ray diffraction measurements were made in order to clear up the ambiguity on the existence of intercalation compound of BN with FeCl_3 . The present work confirmed that the intercalation did not occur when the mixture of BN and FeCl_3 was heated in a sealed tube, independently of temperatures (280–450°C) and durations (1–5 days). Under a certain condition, pink specimens were obtained which were the same ones as those produced by Freeman and Larkindale. However, these were proved to be the hydrolysis product, FeOCl , by the Mössbauer and X-ray measurements.

The Formation of Manganese and Cobalt Ferrites by the Air Oxidation of Aqueous Suspensions and Their Properties. M. Kiyama. *Bull. Chem. Soc. Japan*, **51**, 134 (1978). — Manganese and cobalt ferrites were prepared by the air oxidation of aqueous suspension of $\text{Fe}(\text{OH})_2$ and either $\text{Mn}(\text{OH})_2$ or $\text{Co}(\text{OH})_2$ at 50–80°C. In alkaline suspensions, all the metal ions are transformed into spinel ferrites, $\text{M}_x\text{Fe}_{3-x}\text{O}_4$ (M=Mn or Co), by a suitable combination of the oxidation temperature and the concentration of the excess NaOH. Both manganese and cobalt ferrites consist of ferromagnetic particles (ferrite(A)) when x is smaller than 1.3, nonferromagnetic particles (ferrite(B)) when x is larger than 2, and mixtures of the two in the intervening range. The contents of Mn or Co, both in a solid solution of hydroxides, $\text{M}_{x/3}\text{Fe}_{1-x/3}(\text{OH})_2$, and in ferrite, increase with the progress of the formation of the ferrite(A) caused by oxidation. The formation of the ferrite(B) begins when x in the solid solution reaches 2. Each particle in the ferrite(A) is less homogeneous in comparison with that in the ferrite prepared by a solid-state reaction, although with the same composition. The difference in the homogeneity causes the essential difference in magnetic properties.

Is the Surface of Iron Ferromagnetic? T. Shinjo. *Hyomen (Surface)*, **15**, 678 (1977), in Japanese. — Review.

Magnetic Properties of $\text{Fe}_x\text{V}_{1-x}\text{O}_2$ ($0 < x < 0.05$). K. Kosuge, Y. Ueda, S. Kachi, T. Shinjo, T. Takada, and M. Takano. *J. Solid State Chem.*, **23**, 105 (1978). — The magnetic properties of the $\text{Fe}_x\text{V}_{1-x}\text{O}_2$ system ($0 < x < 0.05$) were investigated by magnetic susceptibility, magnetization, and also by Mössbauer effect measurements. As a result, it is confirmed that the magnetic properties are very similar to those of the $\text{Cr}_x\text{V}_{1-x}\text{O}_2$ system previously studied. At lower temperatures, the exchange-coupled cluster model can well explain the results obtained in this experiment.

Magnetic Properties of $\text{FeSn}(\text{OH})_6$ and Its Oxidation Product, $\text{FeSn}(\text{OH})_5$. N. Nakayama, K. Kosuge, S. Kachi, T. Shinjo, and T. Takada. *Mat. Res. Bull.*, **13**, 17 (1978). — $\text{Fe}^{2+}\text{Sn}^{4+}(\text{OH})_6$ is oxidized in air. As the oxidation product, new compound $\text{Fe}^{3+}\text{Sn}^{4+}\text{O}(\text{OH})_5$ was confirmed. $\text{Fe}^{3+}\text{Sn}^{4+}\text{O}(\text{OH})_5$ has a same structure as that of $\text{FeSn}(\text{OH})_6$. Magnetic properties of these two compounds are investigated; $\text{FeSn}(\text{OH})_6$ is paramagnetic down to 1.4 K, $\text{FeSnO}(\text{OH})_5$ shows an antiferromagnetic order around at 4.2 K.

Preparation and Characterization of Stoichiometric CaFeO₃. Y. Takeda, S. Naka, M. Takano, T. Shinjo, T. Takada, and M. Shimada. *Mat. Res. Bull.*, **13**, 61 (1978). — Stoichiometric CaFeO₃ was prepared and was characterized by crystallographic, magnetic and electrical measurements. A slight tetragonal distortion from the ideal cubic perovskite structure was found. The tetramolecular unit cell has $a=5.325(3)$ Å and $c=7.579(5)$ Å. The susceptibility showed a maximum at about 115 K and the temperature dependence of electrical resistivity changed from metallic to semiconductive in the vicinity of the magnetic transition temperature. These indicate a phase transition from the metallic-paramagnetic (the high-temperature phase) to the semiconductive-antiferromagnetic phase. The Mössbauer spectra indicated that a charge disproportionation $2\text{Fe}^{4+} \rightarrow \text{Fe}^{3+} + \text{Fe}^{5+}$ associates with the transition.

Surface Magnetic Moment of Fe by Mössbauer Effect. T. Shinjo, S. Hine, and T. Takada. *Proc. 7th Intern. Vac. Congr. & 3rd Intern. Conf. Solid Surfaces*, 2655 (1977). — Very thin Fe films (16, 24, 32 and 60 Å) sandwiched with MgF₂ layers were prepared by UHV deposition and the Mössbauer absorption spectra were measured at 300 K and 4.2 K with and without external fields. The results suggest that the thin Fe films are completely ferromagnetic and the magnetic moment of Fe atom in the surface contacting with MgF₂ is bigger than the bulk value. On the other hand, very thin Ni films including 5% Fe-57 (16, 32 and 48 Å) showed no appreciable surface effect.

Magnetic Fine Particles. Y. Bando. *Hyomen (Surface)*, **16**, 380 (1978), in Japanese. — Magnetic single domain particles, superparamagnetism, magnetic recording particles and surface magnetism of $\gamma\text{-Fe}_2\text{O}_3$, $\alpha\text{-Fe}_2\text{O}_3$ and Ni(OH)₂ were reviewed.

Reactive Condensation and Magnetic Properties of Iron Oxide Films. Y. Bando, S. Horii, and T. Takada. *Japanese J. Applied Physics*, **17**, 1037 (1978). — Films of iron oxides such as $\alpha\text{-Fe}_3\text{O}_3$ and Fe₃O₄ were prepared by evaporating iron in a low pressure atmosphere of oxygen gas and investigated by X-ray and electron diffraction and Mössbauer effect measurements. The formation range of iron oxides was determined as functions of the substrate temperature and the deposition rate at an oxygen pressure of 4×10^{-4} Torr. The oxide film consisted of fine grains, and the grain size of Fe₃O₄ increased with increase of the film thickness and the substrate temperature. Magnetic properties were investigated. The coercivity was found to increase up to 1000 Oe with oxidation of the as-deposited Fe₃O₄ films. The origin of such high coercivity was briefly discussed.

Reactive Evaporation. S. Muranaka and Y. Bando. *Kagaku (Chemistry)*, **33**, 483 (1978), in Japanese. — Recent research of the thin film deposition by the reactive evaporation method is reviewed. The stress is laid on the deposition mechanism and the factor which influence the film property is summarized.

Chemistry of Magnetic Materials. Y. Bando. *Kagaku to Kogyo (Chemistry and Chemical Industry)*, **30**, 714 (1977), in Japanese. — Review.

Organic Chemistry

Asymmetric Reduction of α -Ketoesters with Sodium Borohydride by Chiral Phase Transfer Catalysts. R. Kinishi, Y. Nakajima, J. Oda, and Y. Inouye. *Agric. Biol. Chem.*, **42**, 869 (1978). — Single and double asymmetric inductions were achieved by the sodium borohydride reduction of α -ketoesters in the presence of chiral phase transfer catalysts. The quaternary ammonium salts with hydroxyl group in the substituent moiety showed the effective catalytic activity. The reduction of (–)-(3*R*)-menthyl benzoylformate gave (3*R*)-menthyl (*S*)-mandelate in contrast to the prediction by the Prelog rule.

Synthesis of Amino Compounds under Phase Transfer Conditions. Y. Nakajima, R. Kinishi, J. Oda, and Y. Inouye. *Bull. Chem. Soc. Japan*, **50**, 2025 (1977). — The phase transfer process was applied to the reaction of organic bromides with azide anion. The reduction of intermediary azide derivatives gave the corresponding amino compounds, benzylamine, glycine, alanine, butyrine, and serine in fairly good yields. Effective catalytic activity was demonstrated by the difference in chemical yields in the case of methyl bromoacetate and ethyl α -bromopropionate. In order to examine the role of phase transfer catalyst, two bromohydrins (methyl β -hydroxy- α -bromopropionate and styrene bromohydrin) were subjected to the present reaction. Methyl β -hydroxy- α -bromopropionate afforded serine exclusively in the presence of 18-crown-6 and tetrabutylammonium bromide, but in the absence of the catalyst a mixture of serine and isoserine was obtained. A different regioselectivity was observed in the case of styrene bromohydrin.

The Chemistry on Diterpenoids in 1975. Part-II. E. Fujita, K. Fuji, Y. Nagao, M. Node, and M. Ochiai. *Bull. Inst. Chem. Res., Kyoto Univ.*, **55**, 323 (1977). — This is one of a series of annual reviews on diterpenoids chemistry by the authors. It covers the literatures published between July and December 1975 and also omissions in Part-I.

The Chemistry on Diterpenoids in 1976. E. Fujita, K. Fuji, Y. Nagao, M. Node, and M. Ochiai. *Bull. Inst. Chem. Res., Kyoto Univ.*, **55**, 494 (1977). — This is one of a series of our annual reviews on diterpenoids chemistry. Two hundred and twenty references are cited.

The Chemistry on Diterpenoids in 1977. Part-I. E. Fujita, K. Fuji, Y. Nagao, and M. Node. *Bull. Inst. Chem. Res., Kyoto Univ.*, **56**, 111 (1978). — This is one of a series of our annual reviews on diterpenoids chemistry. It covers the literatures published between January and June 1977, and 125 references are cited.

Tumor Inhibitors Having Potential for Interaction with Mercapto

Enzymes and/or Coenzymes. E. Fujita and Y. Nagao. *Bioorganic Chemistry*, **6**, 287 (1977). — On the basis of extensive informations on *in vivo* metabolism as well as biomimetic reactions using simple SH compounds and some enzymes, numerous chemical functions which react with SH groups are divided into two classes; *i.e.*, one which involves electrophilic addition (EA) to an SH group and the other which features displacement reactions (DR) by the SH group. The known tumor inhibitors are accordingly classified into EA and DR types. Biomimetic reactions of tumor inhibitors with model compounds of SH enzymes (or coenzymes) and with some SH enzymes themselves are described. Finally, as enhancement factors for the antitumor activity, the roles of hydrogen-bonding, neighboring group participation, and effect of ester side chains are introduced. These discussions may be expected to serve in the exploitation of the new SH alkylation antitumor agents.

Synthesis of Gibberellins. E. Fujita and M. Node. *Heterocycles*, **7**, 709 (1977). — This review deals with several works concerning synthesis of gibberellin derivatives, total synthesis of gibberellins, and chemical conversions of natural products into gibberellins.

Alkylation of 1, 3-Oxathian. K. Fuji, M. Ueda, and E. Fujita. *J. Chem. Soc. Chem. Comm.*, 814 (1977). — This communication deals with a preliminary result that reaction of 1, 3-oxathienyl-lithium with halides gives 2-alkyl-1, 3-oxathians.

Terpenoids. Part 41. Reactions of *ent*-Kaurenes and 13 β -Kaurenes with Thallium(III) Nitrate in 1, 2-Dimethoxyethane and a Mutual Allylic Rearrangement of the Allylic Nitrate Products. E. Fujita and M. Ochiai. *J. Chem. Soc. Perkin Trans. I*, 1948, (1977). — The reaction of *ent*-kaur-16-ene or 13 β -kaur-16-ene with thallium(III) nitrate in glyme gave only allylic nitrate products, in high yield. The same reaction with *ent*-kaur-15-ene gave also allylic nitrates and additionally an epoxide and an allylic alcohol. Similar treatment of 13 β -kaur-15-ene afforded the allylic alcohols and ketones; considerable amounts of starting material were recovered. The significance of the differences between these reactions is discussed. A mutual allylic rearrangement of the allylic nitrate products is reported.

Terpenoids. XLII. A Convenient Stereoselective Transformation of 16-Exocyclic Methylene Group into Carboxy Group in *ent*-Kaurene and Its 19-Oic Acid. E. Fujita and M. Ochiai. *Chem. Pharm. Bull.*, **25**, 3013 (1977). — By the two successive oxidative rearrangements using thallium trinitrate, *ent*-kaur-16-ene was stereoselectively converted into *ent*-16 α -kauran-17-oic acid. Further application of these reactions led to a convenient transformation of *ent*-kaur-16-en-19-oic acid into *ent*-16 α -kaurane-17, 19-dioic acid.

Terpenoids. XLIII. Total Synthesis of *rac*-Kaur-16-ene-11 α , 15 α -diol. E. Fujita and M. Ochiai. *Chem. Pharm. Bull.*, **26**, 264 (1978). — Total synthesis of the title compound *via* a sequence of reactions including the Birch reduction of *ent*-14-methoxy podocarpa-8, 11, 13-trien-20-ol and the Claisen rearrangement of *ent*-11 α -

vinylloxypodocarp-8-en-14-on-20-olacetate as the key steps has been accomplished.

Terpenoids. Part 44. Oxidative Rearrangement of 17-nor-13 β -kauran-16-one with Thallium(III) Nitrate. E. Fujita and M. Ochiai. *Can. J. Chem.*, **56**, 246 (1978). — 17-Nor-13 β -kauran-16-one on treatment with thallium(III) nitrate in acetic acid gives an oxidatively rearranged product, 9, 10-*friedo*-17-norkaur-5(10)-en-12-one. On heating in the presence of acid the product compound undergoes rearrangement to give an $\alpha\beta$ -unsaturated ketone, 17-norkaur-9(11)-en-12-one, the structure and stereochemistry of which were established by the total synthesis of its racemate.

New Antibiotics, Trichopolyns A and B: Isolation and Biological Activity. K. Fuji, E. Fujita, Y. Takaishi, T. Fujita, I. Arita, M. Komatsu, and N. Hiratsuka. *Experientia*, **34**, 237 (1978). — Polypeptide antibiotics, trichopolyns A and B, were isolated from the culture broth of *Trichoderma polysporum* (Link ex Pers) Rifai (TMI 60146). Assessment of biological activity of the antibiotics against microorganisms was made.

Efficiently Monitored Reduction of Carboxylic Acids into Alcohols or Aldehydes via 2-Thiazoline-2-thiol Esters by Sodium Borohydride or Di-isobutylaluminium Hydride. Y. Nagao, K. Kawabata, E. Fujita. *J. Chem. Soc. Chem. Comm.*, 330 (1978). — This communication deals with reduction of carboxylic acids into alcohols or aldehydes. Carboxylic acids were converted into their 2-thiazoline-2-thiol esters, which were treated with sodium borohydride or di-isobutylaluminium hydride to give the alcohols or the aldehydes respectively, in good yields.

Intracellular Localization of the Capsaicinoid Synthesizing Enzyme in Sweet Pepper Fruits. K. Iwai, K. Lee, M. Kobashi, T. Suzuki, and S. Oka. *Agric. Biol. Chem.*, **42**, 201 (1978). — The intracellular localization of the capsaicinoid synthesizing enzyme which catalyzes the condensation reaction between 9 to 11 carbon branched fatty acids and vanillylamine in sweet pepper fruits is described.

Reduction by a Model of NAD(P)H. XV. Kinetics for the Reduction of Methyl Benzoylformate. A. Ohno, H. Yamamoto, T. Okamoto, S. Oka, and Y. Ohnishi. *Bull. Chem. Soc. Japan*, **50**, 2385 (1977). — Kinetics for the reduction of methyl benzoylformate with N- α -methylbenzyl-1-propyl-1, 4-dihydronicotinamide in the presence of magnesium perchlorate in acetonitrile at 25°C has been studied. The reaction follows first-order in the model compound, first-order in the substrate, and zero-order in magnesium ion when $[\text{Model}] \ll [\text{substrate}]$, $[\text{Mg}(\text{ClO}_4)_2]$. When $[\text{Model}] = [\text{Mg}(\text{ClO}_4)_2] \ll [\text{Substrate}]$, the kinetics is best explained by a mechanism which involves the formation of a complex between the model and magnesium ion followed by the reaction between the complex and the substrate. It is concluded that magnesium ion activates the model to promote the release of an electron.

RhCl(PPh₃)₃-catalyzed Coupling of Diorganomercurials. K. Takagi, N. Hayama, T. Okamoto, Y. Sakakibara, and S. Oka. *Bull. Chem. Soc., Japan*, **50**, 2741

(1977). — $\text{RhCl}(\text{PPh}_3)_3$ has been proved to be an effective catalyst for the reaction of various diorganomercurials to give such coupling products as conjugated diyne, conjugated diene, biaryl, and alkane in good yields under mild conditions. A probable mechanism including the oxidative addition of organomercurials to a rhodium complex and the subsequent reaction of two oxidative-addition adducts to yield the product was presented.

Reduction by a Model of NAD(P)H. XVI. Effect of Magnesium Ion for the Reduction of Thiopivalophenone. A. Ohno, S. Yasui, K. Nakamura, and S. Oka. *Bull. Chem. Soc. Japan*, **51**, 290 (1978). — Magnesium ion retards the reduction of thiopivalophenone with 1-benzyl-1, 4-dihydronicotinamide (BNAH) in acetonitrile. Kinetics and other investigation have revealed that the retardation is due to the formation of non-reactive complexes, thiopivalophenone· Mg^{2+} and BNAH· Mg^{2+} .

Reduction by a Model of NAD(P)H. XVII. Isotope Effects and Magnesium Ion Catalysis. A. Ohno, S. Yasui, H. Yamamoto, S. Oka, and Y. Ohnishi. *Bull. Chem. Soc. Japan*, **51**, 294 (1978). — The reduction of thiopivalophenone with 1-benzyl-1, 4-dihydronicotinamide (BNAH) gives the same value for kinetic deuterium isotope effect (k_H/k_D) and isotopic distribution in the product (Y_H/Y_D) regardless of the presence or absence of magnesium ion. The reduction of methyl benzoylformate with a BNAH-analog in the presence of magnesium ion also gives similar values for k_H/k_D and Y_H/Y_D . It has been concluded that magnesium ion stabilizes the transition state in the reduction of methyl benzoylformate, whereas an intermediate is stabilized by magnesium ion in the reduction of thiopivalophenone.

Isotope Effect in the Reduction of Trifluoroacetophenone. A. Ohno, H. Yamamoto, T. Okamoto, S. Oka, and Y. Ohnishi. *Chem. Lett.*, 65 (1978). — Kinetic and product isotope effects have been studied for the reduction of α, α, α -trifluoroacetophenone with 1-propyl-1, 4-dihydronicotinamide in acetonitrile in the presence or absence of magnesium perchlorate. It is concluded that the magnesium ion catalyzes the initial electron-transfer process of the reduction.

Synthesis of Aryl Iodides from Aryl Halides and Potassium Iodide by Means of Nickel Catalyst. K. Takagi, N. Hayama, and T. Okamoto. *Chemistry Lett.*, 191 (1978). — Facile synthesis of aryl iodides from aryl halides was reported. NiBr_2 -Zn catalyzed the halogen exchange reaction of aryl bromides with potassium iodide under mild conditions. At elevated temperatures, NiBr_2 - PBu_3 was an effective catalyst.

Alkali-metal Ion Acceleration of the Electron-transfer Reaction between *N*-Propyl-1, 4-dihydronicotinamide and Ferricyanide Ion. T. Okamoto, A. Ohno, and S. Oka. *J. Chem. Soc., Chem. Commun.*, 784 (1977). — Alkali-metal ions caused an acceleration of the reaction between *N*-propyl-1, 4-dihydronicotinamide and $\text{Fe}(\text{CN})_6^{3-}$ in the decreasing order $\text{Cs}^+ > \text{Rb}^+ > \text{K}^+ > \text{Na}^+ > \text{Li}^+ \approx \text{Et}_4\text{N}^+$, which suggests

the acceleration of the electron-transfer process by polarizable alkali-metal ions.

Asymmetric Reduction of Methyl Benzoylformate with a Chiral NAD(P)H-Model Compound. A. Ohno, M. Ikeguchi, T. Kimura, and S. Oka. *J. Chem. Soc., Chem. Commun.*, 328 (1978). — The title reaction with *N*-(*R*)- α -methylbenzyl-1-propyl-2-methyl-4-(*R*)-methyl-1, 4-dihydronicotinamide or its 4-(*S*)-methyl isomer affords methyl mandelate in 97% optical yield and quantitative chemical yield.

Experimental and Theoretical Studies on Protonation of Thioketones. T. Yamabe, S. Nagata, K. Akagi, R. Hashimoto, K. Yamashita, K. Fukui, A. Ohno, and K. Nakamura. *J. Chem. Soc., Perkin Trans. II*, 1516 (1977). — The site of protonation in two classes of thioketones, $(RC_6H_4)_2C=S$ ($R=H$ or OCH_3) and $Bu_2C=S$, was investigated by 1H and ^{13}C nmr spectroscopy. For aromatic thioketones, protonation occurs on the thiocarbonyl carbon from the side of the π -plane, whereas for the aliphatic compound, protonation of the sulfur atom occurs from the side of the σ -plane. Electronic absorption spectra also provide information on sites of protonation in these molecules. Results are discussed in terms of total energies, charge-density distributions, and excitation energies of $R_2C=S$ and its protonated derivative elucidated by semi-empirical SCF-MO calculations in the CNDO/2 approximation.

Reduction by a Model of NAD(P)H. XIX. Mimesis for the Reaction with Glutamate Dehydrogenases. K. Nakamura, A. Ohno, and S. Oka. *Tetrahedron Lett.*, 4593 (1977). — Methyl pyruvate has been converted into methyl *N*-phenylalanine by a combination of Hantzsch ester and aniline in acetonitrile in the presence of lithium perchlorate. The reaction is a model of an enzymic reaction by glutamate dehydrogenases.

Reduction by a Model of NAD(P)H. XX. Dependence of Enantiospecificity on the Conversion of Reaction. A. Ohno, T. Kimura, S. Oka, and Y. Ohnishi. *Tetrahedron Lett.*, 757 (1978). — The enantiospecificity of the reduction of benzoylformate with *N*- α -methylbenzyl-1-propyl-1, 4-dihydronicotinamide in acetonitrile in the presence of Magnesium ion changes dramatically with the change of reductant/magnesium ion ratio and the change of conversion percentage of the reduction.

A Facile Preparation of Benzaldehyde Diaryl Acetals. S. Tanimoto, S. Iwata, T. Imanishi, and M. Okano. *Bull. Inst. Chem. Res., Kyoto Univ.*, 56, 101 (1978). — Several benzaldehyde diaryl acetals were prepared in excellent yields by treating sodium phenolates with benzylidene dichloride in dimethyl sulfoxide under mild conditions. These acetals will be cumbersome to prepare by other synthetic methods.

The Thallium(I) Salt-Catalyzed Formation of Isothiocyanates from Isocyanides and Disulfides. S. Tanaka, S. Uemura, and M. Okano. *Bull. Chem. Soc. Japan*, 50, 2785 (1977). — The reactions of various isocyanides with diacyl disulfides or tetraethylthiuram disulfide occur smoothly in the presence of thallium(I)

acetate and thiocarboxylates in various organic solvents to give the corresponding isothiocyanates in good yields. Lead(II) acetate has an activity almost identical with that of thallium(I), while cadmium(II) and silver(I) acetates and copper(I) oxide show a slightly lower activity than the above thallium and lead salts. An ionic scheme involving a complex formation between the metal salt and one S atom of the disulfide, followed by a nucleophilic attack of isocyanide on the adjacent S atom, is proposed for this reaction. It is revealed that the reaction of isocyanide with one equivalent of thallium(III) thiobenzoate in refluxing chloroform similarly affords a good yield of the isothiocyanate through the above mechanism after the decomposition of the thallium(III) salt to thallium(I) thiobenzoate and dibenzoyl disulfide, rather than through a pathway involving thiothallation (α -addition).

The Reaction of Cyclohexyl Isocyanide with Aromatic Diacyl Disulfides.

S. Tanaka, K. Masue, and M. Okano. *Bull. Chem. Soc. Japan*, **51**, 659 (1978). — The reaction of cyclohexyl isocyanide with dibenzoyl disulfide in toluene at a reflux temperature gives cyclohexyl isothiocyanate, together with some unidentified compounds. Based on the substituent effects on the rate, a probable reaction path is proposed. The distinction between two reactions conducted in the absence and in the presence of soft metal salts is also described.

A Convenient Method for the Introduction of 1, 3-Dithiolan-2-yl Group into Active Methylene Compounds. S. Tanimoto, Y. Matsumura, T. Sugimoto, and M. Okano. *Bull. Chem. Soc. Japan*, **51**, 665 (1978). — The reaction of 2-ethoxy-1, 3-dithiolane with a variety of active methylene compounds in the presence of a zinc chloride catalyst was investigated. By this reaction the introduction of a 1, 3-dithiolan-2-yl group into the active methylene compounds was achieved. Some behavior of the 1, 3-dithiolan-2-yl derivative of ethyl acetoacetate, which is one of the newly obtained compounds, was also briefly examined.

The Reaction of Alkyl Halides with Mercury(II) and Potassium Thioacetates and Selenocyanates. S. Uemura, N. Watanabe, A. Toshimitsu, and M. Okano. *Bull. Chem. Soc. Japan*, **51**, 1818 (1978). — The reactions of alkyl halides with mercury(II) and potassium thioacetates afford alkyl thioacetates (RSCOMe), S_N1 and S_N2 type reactions taking place. In neither case is ROCSMe formed. Reactions with mercury(II) selenocyanate usually give only small amounts of alkyl selenocyanates and/or isoselenocyanates as isolated products except the case of benzyl bromide from which benzyl selenocyanate was obtained almost quantitatively. The ambident reactivity of this salt was revealed to be not so strong as that of mercury(II) thiocyanate. The reaction with potassium selenocyanate is also reported for comparison.

The Reactions of Olefins with Chloromethoxymethane or Dimethoxymethane in Nitriles. Y. Wada, T. Yamazaki, K. Nishiura, S. Tanimoto, and M. Okano. *Bull. Chem. Soc. Japan*, **51**, 1821 (1978). — The Lewis acid-catalyzed reactions of olefins with chloromethoxymethane (CM) or dimethoxymethane (DM) and aliphatic or aromatic nitriles afforded the 1:1:1 adducts and/or their hydrolysis

products in various yields, together with the 1:1 olefin-CM (or DM) adducts. AlCl_3 , FeCl_3 , ZnCl_2 and SnCl_4 were effective catalysts for the reaction with CM, whereas BF_3 and SnCl_4 were effective for that with DM. In the case of cyclohexene, the addition proceeded in the *trans*-manner; *i.e.*, the methoxymethyl group and the nitrile molecule were added to the olefin from opposite sides.

Solvent Incorporation in Bromination of Acetylenes in Alcohols. S. Uemura, H. Okazaki, M. Okano, S. Sawada, A. Okada, and K. Kuwabara. *Bull. Chem. Soc. Japan*, **51**, 1911 (1978). — The reactions of acetylenes with bromine in alcohols at 20–25°C afford dibromodialkoxyalkanes in good yields together with variable amounts of dibromoalkenes. Similar treatment of phenylacetylene with copper(II) bromide gives only bromophenylacetylene and 2-phenyl-1, 1, 2-tribromoethylene, the latter being formed by dibromination of the former with copper(II) bromide.

Diarylmethane Formation in the Reaction of Various Metal Acetates with Alkylbenzenes in the Presence of Perchloric Acid. S. Tanaka, S. Uemura, and M. Okano. *J. Chem. Soc., Perkin Trans. I*, 431 (1978). — Treatment of alkylbenzenes with various metal acetates (Mn^{III} , Fe^{III} , Co^{III} , Cu^{II} , and Pb^{IV}) in acetic acid containing perchloric acid at reflux temperature affords diarylmethanes as main products; Mn^{III} and Fe^{III} acetates are found to be better reagents than the others, and have comparable activity for diarylmethane formation. Reactions with Mn^{III} acetate-perchloric acid differ from those with Fe^{III} perchlorate (reported previously) in the following ways: the presence of oxygen increases the amount of benzylic aldehyde produced in the former and of diarylmethane produced in the latter reaction; both disproportionation and polymerization, which occur in the latter reaction, are minimized in the former case, making the work-up procedure easier.

Nitration of Aromatic Hydrocarbons and *ipso*-Nitrosodemetalation of Arylmetal Compounds in Sodium Nitrite-Trifluoroacetic Acid. S. Uemura, A. Toshimitsu, and M. Okano. *J. Chem. Soc. Perkin Trans. I*, 1076 (1978). — Treatment of aromatic hydrocarbons with sodium nitrite in trifluoroacetic acid affords nitroarenes in high yields in sharp contrast to a report in which aromatic nitration occurred only slightly in almost the same reaction system. Nitrosodemetalation at the *ipso*-position occurs to give nitrosoarenes in good yields by similar treatment of various arylmetal compounds (metal=Hg, Tl, Si, Sn, Pb, or Bi), nitrodemetalation hardly occurring in this case. The former reaction proceeds through attack of NO_2^- , while NO^+ or its carrier N_2O_3 is the attacking species in the latter reaction.

Bromodemetalation of β -Methoxyphenethylthallium(III) Diacetate and β -Methoxyphenethylmercury(II) Acetate with Copper-(I) and -(II) Bromide. Direct Evidence for Alkyl Radicals in Bromodethallation by the Spin Trapping Technique. S. Uemura, A. Toshimitsu, M. Okano, T. Kawamura, T. Yonezawa, and K. Ichikawa. *J. Chem. Soc., Chem. Commun.*, 65 (1978). — Free alkyl radicals have been observed by a spin trapping technique in the bromodethallation

of β -methoxyphenethylthallium diacetate with copper(I) bromide; the species have been shown to be involved in the main course of the reaction.

Nitroxide Radical as a Nuclear Spin Decoupling Reagent. Application to Carbon-13 Nuclear Magnetic Resonance Studies of Organothallium Compounds. I. Morishima, T. Inubushi, S. Uemura, and H. Miyoshi. *J. Am. Chem. Soc.*, **100**, 354 (1978). — A novel use of a stable nitroxide radical as a nuclear spin decoupling reagent in the ^{13}C -NMR spectra of organothallium compounds which are very complicated owing to large ^{13}C -Tl nuclear spin couplings has been reported. The ^{13}C doublet pair with spacing of >150 Hz is decoupled, while that of <150 Hz is not decoupled and rather broadened out by the addition of di-tert-butyl nitroxide (DTBN) radical to simplify the spectrum. This method was applied to cis-exo oxythallation adducts of norbornene, norbornadiene, and benzonorbornadiene to confirm their structures.

Cyclopropenone. R. Breslow, J. Pecoraro, and T. Sugimoto. *Org. Syn.*, **57**, 41 (1977). — The ready procedure for preparation of cyclopropenone is described. As a starting material was used 2, 3-dichloro-1-propene, commercially available and cheap. The olefin was reacted with NBS in methanol to give 1-bromo-3-chloro-2, 2-dimethoxypropane in 41–45% yield. The compound was subjected to a double dehydrohalogenation by reaction with KNH_2 in liquid ammonia at -50° , and the resulting 3, 3-dimethoxy cyclopropenone was collected by distillation *in vacuo* (1–2 mm) in 40–65% yield. The desired cyclopropenone was obtained in 88–94% yield by treatment with a dilute sulfuric acid in methylene chloride, and the compound has b.p. 26° (0.46 mm) and m.p. -29 to 28° . Cyclopropenone prepared in this way is quite pure and suitable for most chemical purposes.

Asymmetric Reduction of Aromatic Ketones Bound in the Chiral Hydrophobic Interior of Sodium Cholate Micelle. T. Sugimoto, Y. Matsumura, T. Imanishi, S. Tanimoto, and M. Okano. *Tetrahedron Lett.*, 3431 (1978). — The micelle formed in solubilization of sodium cholate (NaC), one of bile salts, in water above the critical micellar concentration (*ca.* 8 mM at 20°), can serve as a chemically-organized inclusion aggregate capable of binding aromatic ketones into the chiral interior and attaining to asymmetric induction in the subsequent reduction. When alkyl phenyl ketones of acetophenone, isobutyrophenone and tert-butyl phenyl ketone were reduced by NaBH_4 in the presence of 20–160 eq. moles of NaC, no chirality was introduced into the alcohols. Whereas, in the reduction of 1- and 2-acetonaphthones the optically active alcohols were obtained in respective maximum optical yields of 1.7 and 1.2%. The present finding suggests that a host-guest fitting plays an important role in asymmetric induction by the manner of inclusion into the chiral environment.

Polymer Chemistry

Determination of Compositional Heterogeneities for Acrylonitrile-Styrene Copolymers by Thin-Layer Chromatography. J. Wälchli, T. Miya-

moto, and H. Inagaki. *Bull. Inst. Chem. Res., Kyoto Univ.*, **56**, 80 (1978). — Thin-layer chromatography was applied for determining the compositional heterogeneity of acrylonitrile-styrene (AS) copolymer systems. Good separation according to the composition was achieved by a concentration-gradient development with a binary tetrachloroethane+ethyl acetate. A compositional distribution thus found for a radically prepared high-conversion AS copolymer with an AN-content lower than the azeotropic composition was in good agreement with that calculated from copolymerization kinetics assuming the terminal model. While, a bimodal compositional distribution was obtained for a commercial AS copolymer product which had a higher AN-content than the azeotropic composition.

A Generalization of Fujita's Equation for Sedimentation Equilibrium. H. Suzuki. *Bull. Inst. Chem. Res., Kyoto Univ.*, **56**, 89 (1978). — The formal derivation of a generalized form of Fujita's equation for sedimentation equilibrium on nonideal polydisperse system is described.

A Study on Preferential Solvation on Styrene-Methyl Methacrylate Copolymers of Varying Architecture and Composition by Conventional and Density Gradient Sedimentation Equilibrium Methods. A. Nakazawa, N. Donkai, T. Kotaka, and H. Inagaki. *British Polymer Journal*, 200 (1977). — Preferential solvation in quasiternary systems composed of *p*-xylene (*p*XY), 1, 2-dibromo-1, 1-difluoroethane (DBFE) and styrene (ST)-methyl methacrylate (MMA) copolymers of varying architecture and composition was studied by two ultracentrifugation methods: sedimentation equilibrium in a density gradient and conventional sedimentation equilibrium. The preferential solvation parameters were estimated for the systems containing alternating, statistical and block copolymers as well as polymethyl methacrylate (PMMA) and polystyrene (PST). Virtually no solvation was observed by PST, while significant solvation of DBFE to MMA units took place. For alternating and statistical copolymers the solvation parameter is approximately the composition average of those of PST and PMMA, although a slight but distinct difference between those of the alternating and statistical copolymers was observed. However, in block copolymers of either PST-PMMA or PMMA-PST-PMMA type of high PST content, it appears that the solvation of DBFE to PMMA-blocks is suppressed by the presence of PST-blocks.

On the Second Virial Coefficient for Solutions of Polystyrene Mixtures. H. Suzuki. *British Polymer Journal*, 222 (1977). — Light scattering measurements were carried out on several standard polystyrenes and their binary mixtures in benzene and in 2-butanone. Their second virial coefficients, B_2 , were determined as a function of the polymer composition. It was revealed that for some pairs of mixtures whose components differ greatly in size, a minimum in B_2 is observed, whereas a maximum is expected theoretically. The reasons for this phenomenon are discussed and interpreted in terms of the characteristics of the samples in solution and by considering the non-negligible contribution of the attractive forces.

On the Association Phenomena of Poly(methyl methacrylate) in Nonpolar

Theta Solvents. H. Suzuki, T. Hiyoshi, and H. Inagaki. *J. Polym. Sci.: Polymer Symposia*, **61**, 291 (1977). — On a sample of poly(methyl methacrylate) prepared by an anionic polymerization technique with sodium biphenyl in tetrahydrofuran at -78°C , abnormal cloud-point curves in nonpolar theta solvents, *p*-xylene, and carbon tetrachloride were observed. The effect of solvent polarity on precipitation behavior of the sample solutions was examined. It is found that the more polar the solvent used, the more normal the cloud-point curve becomes. Osmometry on the sample solutions in *p*-xylene yielded much higher molecular weights than those obtained in a good solvent (toluene) and in a polar theta solvent (acetonitrile). The results obtained show that poly(methyl methacrylate) molecules prepared in this manner are liable to associate with each other in nonpolar media. This feature is considered to be responsible for the observed anomalies in the cloud-point curves. This type of association is discussed and compared with the other two kinds of association phenomena reported in the literature.

Conformation of Block Copolymers in Dilute Solution. The Molecular Dimension/Block Architecture Relationships. T. Tanaka, T. Kotaka, K. Ban, M. Hattori, and H. Inagaki. *Macromolecules*, **10**, 960 (1977). — Conformational properties of AB di- and BAB triblock copolymers in dilute solution were examined by three different methods including Monte Carlo calculations on a self-avoiding lattice walk, light-scattering measurements with solvents isorefractive for the B blocks, and intrinsic viscosity measurements in different solvents. Polymer samples used were a series of anionically prepared polystyrene (PS)-poly(methyl methacrylate) (PM) diblock and PM-PS-PM triblock copolymers. Emphasis was placed on elucidating the difference between the two copolymers in the effects of heterosegmental interactions on their molecular dimensions. The main conclusions obtained were as opposed to the diblock copolymer case, the central A block in a BAB copolymer is appreciably more expanded than an identical A homopolymer; and the overall dimension of a triblock copolymer is generally larger than that of its diblock equivalent. Together with some calculative and experimental results on a random (statistical) copolymer, it was deduced that copolymer dimension generally becomes larger with the increase of block number when compared at common molecular weight and composition, thus a diblock copolymer having the smallest dimension, and a random copolymer the largest dimension. However, the molecular weight dependence of chain dimension was essentially different between random and block copolymers.

Block Copolymer Micelles in Dilute Solution. T. Kotaka, T. Tanaka, M. Hattori, and H. Inagaki. *Macromolecules*, **11**, 138 (1978). — A light-scattering study was carried out to examine the micelle-forming behavior of polystyrene (PS) and poly(methyl methacrylate) (PMMA) block copolymers of SM-diblock and MSM-triblock types in toluene (TOL)-*p*-cymene (*p*CY) mixture. Both solvents are (nearly) isorefractive to PMMA and good solvents to PS, but *p*CY is a nonsolvent to PMMA. Upon increasing *p*CY content, micelles are formed through the aggregation of (nearly invisible) PMMA blocks. Their morphologies are different depending on *p*CY content, the type of block copolymers involved, *etc.* In SM-diblock copolymer systems with

intermediate p CY content, spherical-shape micelles with a PMMA core, and PS fringes appear to be formed. A theoretical particle scattering function was derived for such a spherical micelle model and compared with the experiments. The fringe PS chains appear to be considerably expanded as compared with the equivalent precursor PS chains, and a substantial extent of PS-PMMA intermixing must have been taking place. At higher p CY content regions, more extended ellipsoidal or cylindrical-shape micelles appear to be present. On the other hand, an MSM-triblock system exhibits in the light-scattering Zimm plot rectilinear scattering envelopes, which suggests the existence of network-like or highly branched-type micelles through the successive aggregation of two PMMA side blocks in the molecules.

Ultracentrifuge Study of Critically Branched Polycondensates, 4. C. G. Leonis, H. Suzuki, and M. Gordon. *Makromol. Chem.*, **178**, 2867 (1977). — Model polycondensates of 1, 10-decanediol and 1, 3, 5-benzenetriacetic acid stabilized by means of diazodiphenylmethane and ketene are utilized to extend further our understanding of the critically branched state and to investigate possible contributions of the ultracentrifuge to the study of highly polydisperse macromolecules in non-ideal, dilute solutions. By way of computerized curve fitting, the concentration gradient curve is obtained from its concentration profile in the ultracentrifuge cell. From this the weight average molecular weight \bar{M}_1 is calculated by the hinge point method. It is also confirmed that values of the two next higher moments of the molecular weight distribution, viz. $\bar{M}_{2/1}$ and $\bar{M}_{3/2}$ (*i.e.* M_z and M_{z+1}) can hardly be distinguished from infinity for these samples. Application of the hinge point method to systems of high polydispersity is found both theoretically and experimentally to furnish M_1 after a dual extrapolation of the measured \bar{M}_1^{app} against the generalized speed parameter λ and the initial concentration c^0 . It is found theoretically that for estimation of the higher molecular weight moments, plots of $\bar{M}_1^{app} \bar{M}_{2/1}^{app}$ and $\bar{M}_1^{app} \bar{M}_{2/1}^{app} \bar{M}_{3/2}^{app}$ (not merely $\bar{M}_{2/1}^{app}$ and $\bar{M}_{3/2}^{app}$) must be extrapolated against the same variables, *i.e.*, λ and c^0 . The quantitative results thus obtained are discussed in the context of previous results on these materials. They are compared with the classical theory for random f -functional polycondensates and statistical cut-off effects on the high molecular weight tail of distribution and assessed.

A Small-Angle Neutron Scattering Study on Poly(ethylene oxide) Crystals. G. Allen and T. Tanaka. *Polymer*, **19**, 271 (1978). — Small-angle neutron scattering measurements were made on poly(ethylene oxide) (PEO) crystallized from the melt. Samples with the deuterated species (DPEO) as a matrix present distinct Bragg peaks from which the lamella spacings can be determined. As a result of strong void-scattering, quantitative analysis of the low-angle regime of these scattering curves is not possible. Samples with the protonous species as a matrix, for which void-scattering is expected to be negligibly small, present unusual scattering curves indicating that they consist of two components, *i.e.*, the intramolecular and intermolecular interference terms. A quantitative analysis of these curves indicates: (1) the solute DPEO molecules are embedded in the crystalline structure of the matrix, assuming rod-like conformations but (2) forming essentially homogeneous aggregates of a few to tens

of the DPEO molecules, depending on the crystallization temperature and the DPEO concentration; (3) the DPEO molecules or aggregates are distributed in space in a non-random manner that corresponds to the presence of inhomogeneous 'domains' having root-mean-square radii of about 250 Å, and each containing about 100 DPEO molecules.

Interaction of Wool Kerateine and Its Derivatives with Heavy Metal Ions. 1. Preparation and Properties of Crosslinked Kerateine-Gels. T. Miyamoto, M. Sugitani, H. Ito, T. Kondo, and H. Inagaki. *Sen-i-Gakkaishi (Journal of the Society of Textile and Cellulose Industry, Japan)*, **34**, 50 (1978), in Japanese. — Chemical processings of waste wool fiber to prepare solid gel-particles (crosslinked kerateine gels), and their basic characteristics as adsorbent for heavy metal ions were investigated. A series of kerateine gels having different thiol(SH)-contents were obtained by gentle oxidation of kerateines which were brought into solution by reducing disulphide bonds of wool fiber. The oxidation was made by dialyzing the kerateine solution against water.

The kerateine gels showed very high uptakes of metal ions, specific to Hg^{2+} , from aqueous media in comparison with those by commercially available adsorbents and native wool. In acid media, a relation was found between the SH-content and Hg^{2+} uptake: the uptake increased with increasing SH-content. The Hg^{2+} uptakes strongly depended on the pH of the media, showing a maximum around pH 2.5 and then a gradual increase in the uptake at pH values higher than 5. The adsorption isotherm did obey the Freundlich equation in acid media but not in alkaline media in a range of lower Hg^{2+} concentrations.

High-Molecular-Weight Fraction of Low-Sulfur S-Carboxymethyl Kerateine: H. Ito, T. Miyamoto, and H. Inagaki. *Sen-i-Gakkaishi (Journal of the Society of Textile and Cellulose Industry, Japan)*, **34**, 57 (1978), in Japanese. — Low-sulfur S-carboxymethyl kerateine (SCMKA) contains a fraction having higher molecular weights than 10^5 as revealed by gel filtration in 8M urea solution, and this fraction has been considered as an aggregate of one of the major components of SCMKA, Component 7. The high-molecular-weight fraction was successfully isolated from SCMKA into two subfractions on a preparative scale by use of Sepharose CL-6B gels. Two major components of SCMKA, *i.e.*, Component 7 and 8, were prepared by fractional precipitation method. It was found that the amino acid compositions of the high-molecular-weight fractions were almost identified with that for Component 7, and further that their molecular weights were 12×10^4 and 18×10^4 . However, a series of experiments showed that any aggregate of Component 7 and 8 or each one of them alone could not be formed in 8M urea solution at pH 7.4. In connection with the multimerization of Component 7, intermolecular crosslinkages due to cystine and lanthionine residues were examined in different manner. It is pointed out that the presence of lanthionine residues in the high-molecular-weight fraction might be most closely related to this problem.

Rheology of Copolymer Solutions V. A Solution of an SB Block Copoly-

mer in 1-Chlorohexadecane. K. Osaki, B. Kim, and M. Kurata. *Bull. Inst. Chem. Res., Kyoto Univ.*, **56**, 56 (1978). — The nonlinear viscoelasticity was studied for a 20% solution of a styrene-butadiene diblock copolymer in 1-chlorohexadecane, which was a non-solvent for the polystyrene block at low temperatures in the range 15–70°C of rheological measurements. At temperatures higher than 50°C, the rheological properties were similar to those of homopolymer solutions. At 40°C, the viscosity at low rates of shear was affected by the flow history. The viscosity measurement at this temperature was subjected to a large error of unknown origin. At temperatures lower than 30°C, the solution exhibited marked nonlinear rheological behavior even at the lowest strain and rate of shear studied; *e.g.*, 0.14 and 0.0005 s⁻¹, respectively. The rate dependence of the viscosity at relatively low rates of shear could be interpreted in terms of the Casson theory based on the concepts of the thread-like sequence structures of hard polystyrene domains and their destruction due to the stress in the flow. At low temperatures, the shear stress increased in double steps at the start of shear flow of a sufficiently high rate of shear and the strain dependence of the relaxation modulus was very large in the range of shear lower than 1 shear unit. The strain-dependent constitutive equation of Bernstein, Kearsley, and Zapas could describe consistently the qualitative features of the rate dependence of the viscosity, the stress growth at the start of steady flow, and the strain dependence of the relaxation modulus.

Infinite-Dilution Viscoelastic Properties of Fibrinogen and Intermediate Fibrin Polymer. N. Nemoto, F. H. M. Nestler, J. L. Schrag, and J. D. Ferry. *Biopolymers*, **16**, 1957 (1977). — The storage and loss shear moduli, G' and G'' , have been measured for dilute solutions of bovine fibrinogen in 68% aqueous glycerol and of intermediate fibrin polymer in 6 *M* hexamethylene glycol, by the Birnboim-Schrag multiple-lumped resonator apparatus with titanium alloy resonators. The frequency range was 100–5800 Hz, the concentration range 1–6 g/l., and the temperatures 10.0 and 25.0°C. The shear moduli G' and G'' at finite concentration, and the extrapolated intrinsic shear moduli $[G']$ and $[G'']$, as functions of frequency, were compared with the predictions of various molecular theories. For fibrinogen, the frequency dependence agreed quite well with the calculations of Hassager for a trinodular rod as modified for the presence of small amounts of dimeric and trimeric aggregates which were deduced from parallel measurements of oscillatory flow birefringence. It was not possible, however, to distinguish between a linearly rigid configuration and one which is freely jointed at the central nodule. A model of a soft elastic sphere (simulating the cage model of Köppel) appeared to be very unlikely. The relaxation time for a rigid trinodular rod and the longest relaxation time for a jointed trinodular rod, calculated from molecular dimensions on the basis of electron microscope measurements, are somewhat smaller than the corresponding observed values; the discrepancy suggests that the molecule is swollen in solution. For the intermediate polymer (which was formed under conditions where ligation is expected), the frequency dependence agreed quite well with that predicted either for a prolate ellipsoid (Cerf-Scherage-Saito) or for a cylindrical rod (Yamakawa). The relaxation time obtained by fitting to theory agrees quite well with that calculated for a cylindrical rod with molecular dimensions based on a degree of polymerization of 20 and lateral binary association

with staggered overlapping.

Characterization of Group C Meningococcal Polysaccharide by Light-Scattering Spectroscopy. III. Determination of Molecular Weight, Radius of Gyration, and Translational Diffusional Coefficient. Y. Tsunashima, K. Moro, B. Chu, and T. Y. Liu. *Biopolymers*, **17**, 251 (1978). — Group-specific polysaccharides isolated by means of a cetavlon procedure are immunogenic in man and induce protective immunity against meningococcal meningitis. Minute quantities of the polymers in solution can act as vaccines. We now report the first characterization of a fractionated (C-1) group C polysaccharide in 0.4 M KCl and 0.05 M sodium acetate by means of light-scattering spectroscopy. Independent measurements of refractive index increments, absolute scattered intensities, angular scattering intensities and line widths as a function of scattering angles and delay times at different concentrations using incident wavelengths of 632.8 nm from a He-Ne laser and of 488 nm from an argon-ion laser yield information on aggregation properties, molecular weight (M_r), radius of gyration $\langle r_g^2 \rangle_z^{1/2}$, translational diffusion coefficient $\langle D \rangle_z^0$, and second virial coefficients A_2 and B_2 of C-1 polysaccharide.

At relatively high ionic strength (0.4 M KCl + 0.05 M sodium acetate), we obtain for the C-1 polysaccharide in solution $M_r = 5.15 \times 10^5$, $\langle r_g^2 \rangle_z^{1/2} = 345 \text{ \AA}$, $A_2 = 1.25 \times 10^{-4} \text{ ml/g}$, $\langle D \rangle_z^0 = 1.16 \times 10^{-7} \text{ cm}^2/\text{sec}$ with a corresponding Stokes radius of 240 Å and $B_2 = 4.4 \text{ ml/g}$. A_2 and B_2 are the second virial coefficients from intensity- and diffusion-coefficient measurements. The C-1 polysaccharide aggregates in solution and behaves hydrodynamically like random coils. Viscosity and sedimentation studies further confirm our conclusions that the fractionated C-1 polysaccharide aggregates in solution and EDTA can partially break up those aggregates. However, the system remains polydisperse even after adding an excess amount of EDTA. The weight-average molecular weight of the C-1 polysaccharide in solution depends upon ionic strength and exhibits a minimum at $\sim 0.2 \text{ M KCl}$. Finally, viscosity, light-scattering, and sedimentation results all show that the aggregated macromolecular system behaves like random-coiled polymers with no measurable shape factors.

Infinite-Dilution Viscoelastic Properties of Sodium Poly(styrene Sulfonate). R. W. Rosser, N. Nemoto, J. L. Schrag, and J. D. Ferry. *J. Polym. Sci.: Polym. Phys. Ed.*, **16**, 1031 (1978). — The storage and loss shear moduli G' and G'' of dilute solutions of two samples of sodium poly(styrene sulfonate) with molecular weights (M) of 3.28×10^5 and 7.8×10^5 have been measured. The Birnboim-Schrag multiple-lumped resonator technique was used in the frequency range 100–8000 Hz, and the intrinsic moduli were obtained by extrapolation to infinite dilution. Measurements were performed over the temperature range from 1.0 to 25.0°C in aqueous solvents containing from 0 to 60% by weight glycerol and from 0.001 to 0.005 M added salt. The large intrinsic viscosities indicated high extension of the polymer, and the frequency dependences of G' and G'' were matched well by hybrid relaxation spectra combining rod-like and coil-like behavior. In a solvent containing 0.001 M sodium ion and no glycerol, the end-over-end rotational relaxation times for the two molecular weights corresponded to proportionality to the 1.7 power of M . With

increasing molecular weight, ionic strength, and/or glycerol concentration, the polyelectrolyte appeared to become less extended, and its behavior more nearly coil-like.

Constitutive Equations for Polymeric Liquids. K. Osaki. *J. Soc. Rheol. Japan*, **5**, 163 (1977), in Japanese. — A review on phenomenological constitutive models for concentrated polymer solutions. The wide applicability as well as the limitation of the strain-dependent model of Bernstein, Kearsley, and Zapas was revealed on the basis of existing data.

Dependence on Molecular Weight of the Chain Expansion Factor of Polystyrene in Dilute Solutions. H. Utiyama, S. Utsumi, Y. Tsunashima, and M. Kurata. *Macromolecules*, **11**, 506 (1978). — Accurate light-scattering and viscosity measurements were made in toluene at 30°C on five polystyrene samples with narrow distribution in molecular weight. In the range of studied molecular weight, 1.3 million to 15.9 million, it was shown that the double logarithmic plot of $\langle S^2 \rangle / M$ against $M^{1/2}$ gave a curve concave downward and that the penetration function ψ in the expression of A_2 decreased with the expansion factor α_s with a tendency to level off. The dependence of α_s on the parameter z of the excluded-volume effect was deduced from the experimental data in a straightforward way by using the slope F in the double logarithmic plot of $(\alpha_s^3 - 1)$ vs. $M^{1/2}$. It was concluded that F , starting from unity at $\alpha_s = 1$, decreased monotonously with α_s . This conclusion was shown to be supported by the data of numerical computations on nonintersecting random walks on three-dimensional lattices. An empirical equation of z was suggested as a function of α_s , which yielded a constant value of 1.28×10^{-3} for $z/M^{1/2}$ for the present polystyrene-toluene system regardless of molecular weight.

Diffusion and Solution of Gases and Vapors in Styrene-Butadiene Block Copolymers. H. Odani, K. Taira, N. Nemoto, and M. Kurata. *Polym. Eng. Sci.*, **17**, 527 (1977). — The diffusion, solution, and permeation behavior of a series of inert gases (helium, argon, nitrogen, krypton, and xenon) in S-B block copolymer films was studied by transient permeability measurements and by the equilibrium desorption method. The morphologies of most of the samples used in the measurements were (a) polystyrene rods dispersed in a polybutadiene matrix and (b) alternating lamellae of styrene and butadiene components. It was indicated, as far as the kinetic nature at lower temperatures is concerned, that the diffusion and permeation processes of gases, except for helium, are governed primarily by behavior in the polybutadiene matrix. At lower temperatures, it was shown that the transient method counts only the mobile penetrant in the polybutadiene matrix, while the equilibrium method counts less diffusive species in the polystyrene domains as well. The diffusion behavior in the copolymer films was compared with that in homopolybutadiene and discussed in terms of two impedance factors: the tortuosity and the chain immobilization factors. From the homopolymer-block copolymer comparison along with results obtained from diffusion experiments using *n*-hexane as the penetrant, it was indicated that segmental motions in the polybutadiene phase in the copolymers are restricted relative to motions in homopolybutadiene. Also, from data on gas sorption in samples of

various styrene contents, involving both S-B block copolymers and binary mixtures with homopolystyrene, it was suggested that the partial mixing of component block chains occurs at the interface between the domains, resulting in rather diffuse domain boundaries.

Rheology of Copolymer Solutions. III. The Linear Viscoelasticity of SBS Block Copolymer Solutions. K. Osaki, B. Kim, and M. Kurata. *Polymer J.*, **10**, 353 (1978). — Linear viscoelastic behavior was investigated for concentrated solutions of a styrene-butadiene block copolymer, that is, a 4-armed star-branched polybutadiene structure with a polystyrene block on each chain end. The effect of varying solvent, concentration c , and temperature T was investigated by applying the method of reduced variables to the shear stresses at the start and on cessation of steady shear flow. When the solvent had a strong solvent power for both the polystyrene and the polybutadiene, the viscoelastic behavior was only slightly different from that in homopolymer solutions. In the case of the 1-chlorohexadecane solvent, the solubility of polystyrene varied much in the temperature range of measurement. In this case, the method of reduced variables with respect to $t-c$ and $t-T$ was not applicable, the viscosity η^0 varied to a very large extent with c and T , and the ratio τ_{max}/η^0 increased with increasing c , where τ_{max} is the maximum relaxation time. The result was tentatively interpreted in terms of a molecular aggregate consisting of a few molecules connected to each other through the hard domains of the polystyrene block solution.

A Crystal-Structural Comparison of Polyethylene with n -Paraffins: I. Effects of the Crystal Surface on the Crystalline Core. A. Kawaguchi. *Bull. Inst. Chem. Res., Kyoto Univ.*, **56**, 68 (1978). — A light was thrown upon the crystal-line structure of polyethylene from a study on the n -paraffins which were both chemically and crystallographically analogous to polyethylene. The (200)₀ spacing increased to various extents as a result of the phase transition of n -C₃₆H₇₄ (from the monoclinic M₀₁₁ crystal to the orthorhombic) or the formation of the mixed crystal of two different n -paraffins in chain length, *i.e.* n -C₃₂H₆₆ and n -C₃₅H₇₂. This spacing increase was caused by the methyl end groups which change their manner of packing at the crystal surface. The smaller lattice spacings were observed in the as-grown polyethylene crystal with larger thickness. Although the thickness of solution-grown crystal was increased by annealing, the spacing increased when the thickness of annealed crystal ranged from 180 Å to 220 Å. The thickness dependence of the lattice spacing in polyethylene was discussed on the basis of two types of effects; (i) a conformational strain to be stored in a fold at the lamellar surface and (ii) the interactions between bulky folds.

Accurate Stigmating of a High Voltage Electron Microscope. O. L. Krivanek, S. Isoda, and K. Kobayashi; *Journal of Microscopy*, **111**, 279 (1977). — To reach the 0.2 nm point-to-point resolution possible with some high voltage electron microscopes, the astigmatism of the objective lens must be compensated to within 5 nm. Due to a number of factors the resolution of the image seen on the viewing screen of the high voltage microscope is, however, quite poor and does not permit

compensation of such accuracy.

We describe a technique for evaluating and correcting the astigmatism that starts from a recorded micrograph of a thin amorphous specimen. The astigmatism is determined from the optical diffraction pattern using a variation of the Thon method. This variation avoids any direct measurement of the radii of the contrast transfer zones, and is extremely rapid and convenient. Adjusting the stigmator coil currents, calibrated in terms of their stigmating power, for zero astigmatism completes the correction in less than 10 min after the recording of the micrograph.

Lattice Imaging of a Grain Boundary in Crystalline Germanium. O. L. Krivanek, S. Isoda, and K. Kobayashi, *Phil. Mag.*, **36**, 931 (1977). — A high-angle tilt grain boundary viewed end-on in a (011) thin crystal of Ge has been imaged with atomic resolution in the Kyoto 500 kV electron microscope. The boundary is shown to consist of alternating columns of five- and seven-membered rings of Ge atoms running along the [011] direction, and to contain no dangling bonds.

Crystalline Structure of Polynosic and Cuprammonium Rayon Treated with Alkali and Acrylonitrile in the Presence of Ethanol. A. Hirai and A. Nakajima. *Bull. Inst. Chem. Res., Kyoto Univ.*, **56**, 49 (1978). — Regenerated celluloses such as polynosic and cuprammonium rayon fibers were cyanoethylated after pretreatment with 5.4 *N* NaOH in a mixture of ethanol and water (volume ratio 30:70), and the crystalline structure of the products was investigated by X-ray method. The influence of cyanoethyl residues at least on the crystalline structure of cellulose was indistinguishable between regenerated cellulose and cotton.

NMR Approach to the Phase Structure of Linear Polyethylene. R. Kitamaru, and F. Horii. *Advances in Polym. Sci.*, **26**, 137 (1978). — The recent studies of the phase structure of linear polyethylene by refined NMR analyses are reviewed. The phase structure of the polymer in various crystalline forms, including bulk-crystals, solution-crystals and drawn fibers, is discussed in terms of different modes of molecular mobilities in a wide range of temperature.

Blood Coagulation Induced by Surface. Y. Ikada. *Hyomen (Surface)*, **15**, 718 (1977), in Japanese. — This review article covers the biochemical mechanism of blood coagulation and the plasmaprotein adsorption on foreign bodies. The adsorption followed by protein denaturation is believed to be the initial event for the blood coagulation on polymeric materials.

Platelet Adhesion and Non-Thrombogenic Materials. Y. Ikada. *Nippon Setchaku Kyokai Shi (Journal of the Adhesion Society of Japan)*, **13**, 264 (1977), in Japanese. — Since the platelet adhesion is an influencing factor in thrombus formation, the representative mechanisms for platelet adhesion on the materials from natural and synthetic polymers are described somewhat in detail. In addition, comparison is made for the degree of platelet adhesion on several polymeric materials which have proved to exhibit relatively good blood-compatibility.

Polyelectrolyte Complex Prepared from Carboxymethylated and Aminoacetalized Derivatives of Poly(vinyl alcohol). M. Hosono, S. Sugii, R. Kitamaru, Y. M. Hong, and W. Tsuji. *J. Applied Polym. Sci.*, **21**, 2125 (1977). — Some physical and chemical properties of an ionic complex made from the weak polyelectrolytes carboxymethylated poly(vinyl alcohol) (PA) and aminoacetalized poly(vinyl alcohol) (PC) are investigated in comparison with those of another ionic complex made from the strong polyelectrolytes sulfated poly(vinyl alcohol) (PSA) and poly(vinyl alcohol) acetalized with diethoxyethyltrimethylammonium (PTC). It was found that when the complex PC-PA was heated at high temperatures, covalent amide bonding took place, whereas no significant change occurred in the case of the PTC-PSA complex. As a result of these structural changes, the degree of swelling of the PC-PA complex in water was markedly decreased, but that of the PTC-PSA complex was not changed by the treatment. The PC-PA complex was insoluble in water and in 1 *N* HCl and 1 *N* NaOH aqueous solutions even if not heat treated, but the PTC-PSA complex was soluble in such acidic and basic aqueous solutions but not in water if heat treated. The PC-PA and PTC-PSA films exhibit good mechanical properties.

Refined NMR Analysis of the Phase Structure of Solution-Crystallized Linear Polyethylene. F. Horii and R. Kitamaru. *J. Polym. Sci., Polym. Phys. Ed.*, **16**, 265 (1978). — Nuclear magnetic resonance (NMR) spectroscopy reveals that solution-grown polyethylene samples have a unique phase structure independent of molecular weight. The lamellar crystallites are composed of about 85% crystalline material with the noncrystalline overlayer as large as 15%. The molecular motion in the overlayer is comparatively hindered and the liquid-like component, which is generally recognized in melt-grown crystals, cannot be produced appreciably, even at 60°C. Such hindered molecular mobility can be understood in terms of a rather restricted conformation of the molecular chains in the noncrystalline overlayer, arising from the special mode of crystallization from dilute solution.

Crystallite Size Determination and Identification of Lamellar Surfaces of Microparacrystallites for Uniaxially and Doubly Oriented Polyethylene Films. K. Kaji, T. Mochizuki, A. Akiyama, and R. Hosemann. *J. Materials Science*, **13**, 972 (1978). — Low density polyethylene (PE) films stretched 4x at 20°C and annealed at 100°C show the well-known SAXS four-point diagrams with a tilting angle of lamellae of 35°. The 7.5 nm thick lamellae consist of rod-like microparacrystallites (mPCs) of 25 nm × 7.2 nm lateral sizes; the long axes of the mPCs are turned around the *c*-axis by 31° from the *b*-axis. The mPCs of each lamella stack together laterally like mono-layers of cigars. After rolling the molten film at room temperature and then annealing at 100°C, a doubly oriented film arises, each half of it, anterior or posterior, producing a monoclinic two-point diagram. These are superimposed in SAXS. The mPCs are oriented in the plane stress field so that their *b*-axis is orthogonal to the stretching direction and parallel to the film surface; their long axes however are again turned as before, but now by 26°. Furthermore their *a*-axis is tilted around the *b*-axis by 8° and the lamellar basal surface tilted against the

b-axis in the opposite direction by 40°. The line profiles of the SAXS reflections give evidence that statistical irregularities of the lamellar surfaces are correlated in the 8° tilted direction or along the chain axis with the neighbouring surfaces by means of ultrafibrillar properties of the lamellar bundles, *e.g.* ribbon-like microfibrillar details of the lamellae. These can be described quantitatively by applying the theory of paracrystals on the superlattice generated by the centres of the mPCs. The lamellar surfaces are approximately parallel to the {523} and {311} netplanes of mPCs for the uniaxially and doubly oriented films, respectively. The conventional theory of mesophases can never describe structures which combine lamellar and fibrillar properties.

The Phase Structure of Polymers and Broad-Line NMR. R. Kitamaru. *Kagaku no Ryoiki (J. Japanese Chemistry)*, **32**, 15 (1978), in Japanese. — Our recent studies of the phase structure of linear polyethylene, polyethylene terephthalate crystallized under various conditions and cellulose fibers mainly by a refined NMR analyses are reviewed.

Heating Effects on the Structure of Polyelectrolyte Complexes Prepared from Carboxymethylated and Aminoacetalized Derivatives of Poly(vinyl alcohol). M. Hosono, S. Sugii, and W. Tsuji. *Kobunshi Ronbunshu*, **34**, 843 (1977), in Japanese. — Polyelectrolyte complexes were prepared from carboxymethylated poly(vinyl alcohol)(**I**) and aminoacetalized poly(vinyl alcohol)(**II**) under various conditions and their structural changes upon heating were investigated by infrared spectroscopy. Films prepared by casting the sodium hydroxide or hydrochloric acid aqueous solutions containing **I** and **II** were simple physical mixtures, but washing of the films with methanol yielded polyelectrolyte complexes having ionic bonds. Heating of the complexes above 120°C gave rise to transformation of the ionic bonds to amide linkages ($-\text{NH}_3^+ : -\text{OOC}- \rightarrow -\text{NH}-\text{CO}- + \text{H}_2\text{O}$). However, when the films made from sodium hydroxide solutions were heated without washing with methanol, no amide but hydrogen bonding due to NH_2 groups was observed. In contrast, amide formation took place on heating the films which were prepared from hydrochloric acid solutions but not subjected to washing with methanol. This may be due to disappearance of hydrochloric acid through heating, resulting in formation of ionic bonds.

Determination of the Elastic Modulus of Polyamide Crystals Along the Chain Axis by X-Ray Diffraction, 1. The α -Form of Nylon-6. K. Kaji and I. Sakurada. *Makromol. Chem.*, **179**, 209 (1978). — Studies were carried out to determine the crystalline elastic modulus E_1 along the chain axis for the α -form of nylon-6 [poly(ϵ -caprolactam)] by X-ray diffraction. To obtain an inherent E_1 value of this polymer the problem was solved that different orders of meridional reflections give different E_1 values. Thus the disagreement was found to be due to the increase of the crystallite size by the applied stress. When corrected for this effect, the values from the 040 and 0.14.0 reflections agreed well with each other. The resulting modulus was 183 GN/m² at 23°C, which was much lower than a theoretically

calculated value of 262.8 GN/m² for the fully extended structure model by *Manley* and *Martin*. This seems to be due to the slight shortening at the amide group of the molecular chain because it was confirmed from the intensity changes of the 040 and 0.14.0 reflections of this polymer by the applied stress that the amide part is more extensible than the polymethylene section.

Judging from similar considerations the previously reported E_1 values for nylon-66 and nylon-6, 10 are valid.

Coupling Reactions between Polystyrene Containing Acyl Chloride Endgroups and Poly(vinyl acetate) Containing Amino Groups at the Chain End or Along the Chain. Y. Ikada, K. Maejima, and H. Iwata. *Makromol. Chem.*, **179**, 865 (1978). — Polystyrene (PS) and Poly(vinyl acetate) (PVAc), both carrying one terminal acyl chloride group, were synthesized by radiation-polymerization in the presence of trichloroacetyl chloride, a chain transfer agent, and the acyl chloride groups of PVAc were converted to amino groups by reacting with excess ethylenediamine. Partial acetalization of poly(vinyl alcohol) with aminoacetaldehyde followed by acetalation of the remaining hydroxyl groups in the polymer yielded PVAc having a number of pendant amino groups distributed along the main chain. Condensation coupling reactions between the acyl chloride and amino groups were carried out in chloroform at room temperature to yield PS-PVAc diblock copolymers and PVAc-PS graft copolymers with many branches of PS. The pure copolymers were isolated from the reaction products by extraction and then characterized by determining chemical compositions and number-average molecular weights.

Chain Transfer in Radical Polymerizations and End Group Content of Resultant Polymers. Y. Ikada, H. Iwata, and S. Nagaoka. *Macromolecules*, **10**, 1364 (1977). — The radical polymerization of vinyl monomers was carried out in the presence of reactive chain transfer agents possessing functional groups and the weight fractions of the resultant polymers bearing functional groups from the transfer agents were determined with a thin-layer chromatographic method. The monomer-chain-transfer agent combination chosen in the present work is styrene-trichloroacetyl chloride and methyl methacrylate-2-aminoethanethiol hydrochloride. The chain-transfer polymerizations were expected to produce polystyrene with an acyl chloride end group and poly(methyl methacrylate) with an amino end group in a high yield. The end group content of resultant polymers determined by the thin-layer chromatography was in both cases in good agreement with that predicted from the polymerization kinetics, suggesting that the thin-layer chromatography can be effectively applied to the end group determination.

Physico-Chemical Properties of Hydrogels. Y. Ikada and F. Horii. *Nippon Kagakusen-i Kenkyusho Koenshu*, **34**, 1 (1977), in Japanese. — A hydrogel is defined as a polymeric material which exhibits the ability to swell in water and retain a significant fraction (e.g. >20%) of water within its structure. Recently this material has attracted attention in the field of biomedical materials because of its excellent biocompatibility. A semipermeable membrane for ultrafiltration can be prepared also from the hydrogel.

We prepared hydrogels by crosslinking of poly(vinyl alcohol) and other water-soluble polymers under various conditions and studied some fundamental properties as a function of the equilibrated water content. Tensile strength, water structure and water permeability were determined for the hydrogels different in the starting polymer and the water content.

Effect of Ethanol on Alkali and Acrylonitrile Treatments for Cotton.

A. Hirai, A. Nakajima, and W. Tsuji. *Polym. J.*, **10**, 247 (1978). — Cotton fibers were pretreated with 5.4 *N* sodium hydroxide in an ethanol-water (volume ratio, 30:70) mixture and then cyanoethylated with acrylonitrile. The crystalline structure of the cyanoethylated cotton fibers was investigated by the X-ray method and compared with that of the cotton fibers, pretreated with 5.4 *N* aqueous sodium hydroxide and cyanoethylated under the same conditions. The presence of ethanol in the sodium hydroxide solution resulted in the increased accessibility of cellulose and a remarkable broadening of the X-ray profile. Cotton fabrics were also treated with alkali-acrylonitrile in the presence of ethanol; their physical properties are discussed.

Structure of Decrystallized Cotton Prepared in Fiber Form by Alkali and Acrylonitrile Treatments.

A. Hirai, M. Hosono, and W. Tsuji. *Sen-i Gakkaishi (J. Soc. Fiber Science and Technology)*, **34**, T-6 (1978). — The moisture regain and the crystalline structure of partially cyanoethylated cotton fibers were examined in comparison with the results on the cotton fabrics. Cotton was treated with acrylonitrile at 20°C and 0°C after immersing in 18 wt% NaOH aqueous solution at 15°C and -5°C, respectively. A greater effect of cyanoethyl residue to retain highly decrystallized state of the treated cotton fibers was observed in the cyanoethylation at 0°C and the fibers showed greater moisture regain. On the contrary, the effect of temperature on the treatment for cotton fabrics was not so sensitive as in the case of fibers. Such factors as textile structure in fabrics, temperature in alkali-pretreatment and cyanoethylation, and the rate of diffusion of acrylonitrile were considered as the causes of the discrepancy.

Properties of Decrystallized Cotton Prepared by Alkali-Acrylonitrile Treatment.

A. Hirai, W. Tsuji, and M. Hosono. *Sen-i Gakkaishi (J. Soc. Fiber Science and Technology)*, **34**, T-82 (1978). — Highly accessible and decrystallized cotton can be prepared by cyanoethylation with acrylonitrile after pretreatment with swelling agents. In this research, cotton fabrics with or without chemical crosslinkages were treated with acrylonitrile after impregnation with 5.4 *N* aqueous sodium hydroxide solution, and some physical properties of the treated cotton were examined. Fairly high moisture regains were obtained. The abrasion resistance of cotton fabrics was increased by the alkali-acrylonitrile treatment. The tensile strength, elongation and moisture regain of treated fabric were increased when the alkali-acrylonitrile treatment was given to chemically crosslinked cotton fabrics, although a small loss in dry crease recovery was caused.

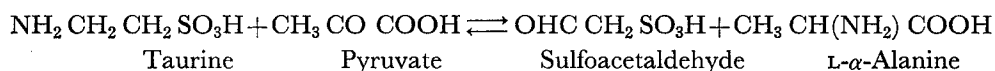
NMR Studies of the Structure of Fibers. R. Kitamaru and F. Horii. *Sen-i*

Gakkaishi (J. Soc. Fiber Science and Technology), **34**, P-103 (1978), in Japanese. — Our recent NMR studies are reviewed on the phase structure of synthetic and natural fibers such as polyethylene, nylon-6, polyethylene terephthalate, and celluloses.

Biochemistry

Properties of Crystalline ω -Amino Acid: Pyruvate Aminotransferase of *Pseudomonas* sp. F-126. K. Yonaha, S. Toyama, M. Yasuda, and K. Soda. *Agric. Biol. Chem.*, **41**, 1701 (1977). — ω -Amino acid: pyruvate aminotransferase, purified to homogeneity and crystallized from a *Pseudomonas* sp. F-126, has a molecular weight of 172,000 or $167,000 \pm 3,000$ as determined by the gel-filtration or sedimentation equilibrium method, respectively. The enzyme catalyzes the transamination between various ω -amino acids or amines and pyruvate which is the exclusive amino acceptor. α -Amino acids except L- α -alanine are inert as amino donor. The Michaelis constants are 3.3 mM for β -alanine, 19 mM for 2-aminoethane sulfonate and 3.3 mM for pyruvate. The enzyme has a maximum activity in the pH range of 8.5~10.5. The enzyme is stable at pH 8.0~10.0 and at up to 65°C at pH 8.0. Carbonyl reagents strongly inhibit the enzyme activity. Pyridoxal 5'-phosphate and pyridoxamine 5'-phosphate reactivate the enzyme inactivated by carbonyl reagents. The inhibition constants were determined to be 0.73 mM for D-penicillamine and 0.58 mM for D-cycloserine. Thiol reagents, chelating agents and L- α -amino acids showed no effect on the enzyme activity.

ω -Amino Acid: Pyruvate Aminotransferase in Bacteria, Part I. Taurine Aminotransferase Reaction. S. Toyama, K. Yonaha, M. Yasuda, and K. Soda. *Amino Acid-Nucleic Acid*, **37**, 13 (1978), in Japanese. — The activity of taurine: pyruvate aminotransferase was generally distributed in bacteria of pseudomonad, though the enzyme activity was not detected in strains of *Agrobacterium*, *Achromobacter*, *Alcaligenes*, *Flavobacterium*, *Escherichia*, *Aerobacter*, *Proteus*, *Brevibacterium*, *Bacillus* and *Bacterium*. A high activity of the aminotransferase was found in the cell-free extract of *Pseudomonas* sp. F-126 isolated from soil, and the bacterium was chosen for characterization for the enzymatic reaction. The enzyme was produced inducibly by addition of β -alanine to the growth medium with a maximum at 0.3~0.5%. The enzyme was catalyzed reversibly the transamination between taurine and pyruvate producing sulfoacetaldehyde and L- α -alanine, respectively, as follow.



Spectrophotometric assay methods for the aminotransferase activity with 2, 4-dinitrophenylhydrazine and *o*-aminobenzaldehyde were also presented.

Bacterial ω -Amino Acid: Pyruvate Aminotransferase, Part II. Purification and Enzymologic Properties. S. Toyama, K. Yonaha, M. Yasuda, and K. Soda. *Amino Acid-Nucleic Acid*, **37**, 21 (1978), in Japanese. — ω -Amino acid: pyruvate

aminotransferase, purified to homogeneity and crystallized from a *Pseudomonas* sp. F-126, has a molecular weight of 172,000 or $167,000 \pm 3,000$ as determined by the gel-filtration or sedimentation equilibrium method, respectively. The enzyme exhibits absorption maxima at 280 and 345 nm and a shoulder at 390~400 nm with molecular absorption coefficients of 174,000, 168,000, and 14,000, respectively. The enzyme catalyzes the transamination between various ω -amino acids and pyruvate which is the exclusive amino acceptor. α -Amino acids except L- α -alanine are inert as amino donor. The Michaelis constants are 3.3 mM for β -alanine and pyruvate, and 19 mM for taurine. The enzyme has a maximum activity in the pH range of 8.5~10.5. The enzyme is stable at pH 8.0~10.0 and at up to 65°C at pH 8.0. Carbonyl reagents strongly inhibit the enzyme activity. Pyridoxal-5'-phosphate and pyridoxamine-5'-phosphate reactivate the enzyme inactivated by carbonyl reagents. Thiol reagents, chelating agents and L- α -amino acids showed no effect on the enzyme activity.

Spectrophotometric Determination of L-Lysine with L-Lysine; α -Ketoglutarate ϵ -Aminotransferase. K. Soda, T. Hirasawa, and T. Fukumura. *Anal. Biochem.*, **87**, 283 (1978). — A simple and sensitive technique with bacterial L-lysine: α -Ketoglutarate ϵ -aminotransferase for the determination of L-lysine (or L-ornithine) has been presented. This method involves a transamination of L-lysine with α -Ketoglutarate to produce Δ^1 -piperidine-6-carboxylate and the spectrophotometric determination of this product with *o*-aminobenzaldehyde.

2-Nitropropane Dioxygenase from *Hansenula mrakii*: Generation and Participation of Superoxide Anion in the Reaction. K. Soda, T. Kido, and K. Asada. *Biochemical and Medical Aspects of Active Oxygen, Tokyo*, 119 (1977). — 2-Nitropropane dioxygenase from a yeast, *Hansenula mrakii*, is a nonheme iron flavoprotein which catalyzes the following reaction.



The enzyme, which has been purified to homogeneity, is unique in that it incorporates 2 atoms of oxygen molecule into two molecules of the same acceptor. The enzyme has a molecular weight of approximately 62,000 and consists of two subunits non-identical in molecular weight (39,000 and 25,000). The enzyme exhibits absorption maxima at 274, 370, 415, and 440 nm and a shoulder at 470 nm, and contains 1 g-atom of nonheme iron and 1 mol of FAD/mol of enzyme protein as prosthetic groups. The enzyme-bound FAD is reduced by 2-nitropropane under anaerobic conditions, but the enzyme-bound Fe^{3+} is not affected.

The enzyme activity is significantly inhibited by superoxide dismutase and various scavengers of O_2^- , such as cytochrome *c*, epinephrine, NADH, tiron, and thiols. The reduction of cytochrome *c*, and the oxidation of epinephrine and NADH do not occur in the presence of superoxide dismutase, or in the absence of 2-nitropropane and oxygen. The enzyme catalyzes the formation of nitrite from 2-nitropropane by KO_2 even under anaerobic conditions. These findings indicate the generation of O_2^- and its participation in the oxygenation of 2-nitropropane. One mole of NADH is bound to 1 mol of the enzyme and the *pro*-R hydrogen of bound NADH is mainly

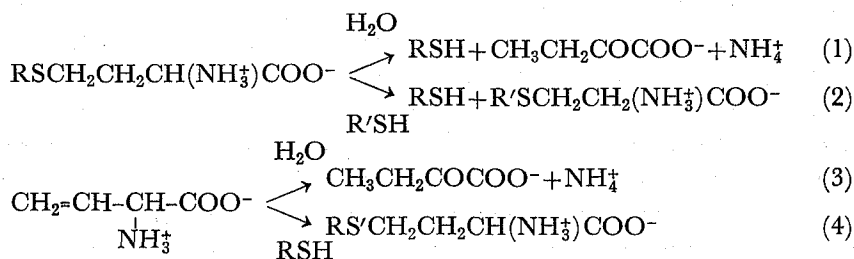
transferred to O₂-formed enzymically or given exogenourly. Thus, the diastereotopic hydrogen of NADH is discriminated by the enzyme, though not completely.

Properties of Taurine α -Ketoglutarate aminotransferase of *Achromobacter superficialis*. Inactivation and Reactivation of Enzyme. S. Toyama, H. Misono, and K. Soda. *Biochim. Biophys. Acta*, **523**, 75 (1978). — The activity of taurine: α -ketoglutarate aminotransferase (taurine: 2-oxoglutarate aminotransferase, EC 2.6.1.55) from *Achromobacter superficialis* is significantly diminished by treatment of the enzyme with (NH₄)₂SO₄ in the course of purification, and recovered by incubation with pyridoxal phosphate at high temperatures such as 60°C. The inactive form of enzyme absorbing at 280 and 345 nm contains 3 mol of pyridoxal phosphate per mol. The activated enzyme contains additional 1 mol of pyridoxal phosphate with a maximum at 430 nm. This peak is shifted to about 400 nm as a shoulder by dialysis of the enzyme, but the activity is not influenced. The inactive form is regarded as a partially resolved form, *i.e.* a semiapoenzyme. The enzyme catalyzes transamination of various ω -amino acids with α -ketoglutarate, which is the exclusive amino acceptor. Hypotaurine, DL- β -aminoisobutyrate, β -alanine and taurine are the preferred amino donors. The apparent Michaelis constants are as follows; taurine 12 mM, hypotaurine 16 mM, DL- β -aminoisobutyrate 11 mM, β -alanine 17 mM, α -ketoglutarate 11 mM and pyridoxal phosphate 5 μ M.

Deamination and γ -addition Reactions of Vinylglycine by L-methionine γ -lyase. N. Esaki, T. Suzuki, H. Tanaka, K. Soda, and R. R. Rando. *FEBS Letters*, **84**, 309 (1977). — Recently we have purified L-methionine γ -lyase to homogeneity from *Pseudomonas putida* (*Ps. ovalis*), and showed that the enzyme catalyzes α , γ -elimination and γ -replacement reactions of L-methionine and its derivatives, and also α , β -elimination and β -replacement reactions of *S*-substituted-L-cysteines [1, 2]. A Schiff base between pyridoxamine 5'-phosphate and 2-keto-3-butenic acid is regarded as a key intermediate in the α , γ -elimination (1) and γ -replacement (2) reactions as reviewed by Snell and Di Mari [3], and Davis and Metzler [4].

The conversion of vinylglycine into α -ketobutyrate was demonstrated with serine-threonine dehydratase of sheep liver [5] and tryptophan synthase of *Escherichia coli* [6]. Cooper *et al.* [7] reported the γ -addition reaction of vinylglycine by L-amino acid oxidase snake venom.

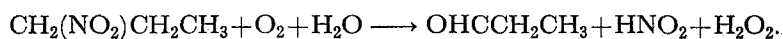
The present investigation was undertaken to elucidate whether vinylglycine can be a substrate for deamination (3) and γ -addition (4) reactions by L-methionine γ -lyase.



Purification and Properties of a Novel Enzyme, L- α -Amino- ϵ -Caprolactamase from *Cryptococcus laurentii*. T. Fukumura, G. Talbot, H. Misono, Y. Teramura, K. Kato, and K. Soda. *FEBS Letters*, **89**, 298 (1978). — A novel synthetic process of L-lysine from DL- α -amino- ϵ -caprolactam with almost 100% yield has been established [1]. This process is composed of two new enzymatic reactions, the selective hydrolysis of L- α -amino- ϵ -caprolactam to L-lysine, and the racemization of α -amino- ϵ -caprolactam, which proceed in the same vessel. The L- α -amino- ϵ -caprolactam hydrolyzing enzyme (L- α -amino- ϵ -caprolactamase (EC 3.5.2.)) has been found in the cells of *Cryptococcus laurentii* and other yeasts [2, 3]. α -Amino- ϵ -caprolactam racemase has been found in the cells of *Achromobacter obae* and other bacteria [4]. Both enzymes were partially purified from *C. laurentii* and *A. obae*, respectively [5, 6].

In this paper, we describe the purification of the new amidohydrolase from *C. laurentii* to homogeneity and some of its properties.

Purification and Properties of Nitroalkane Oxidase from *Fusarium oxysporum*. T. Kido, K. Hashizume, and K. Soda. *J. Bact.*, **133**, 53 (1978). — A nitroalkane-oxidizing enzyme, which was inducibly formed by addition of nitroethane to the medium, was purified to homogeneity from an extract of *Fusarium oxysporum* (IFO 5942) with an overall yield of about 20%. The enzyme catalyzed the oxidative denitration of 1-nitropropane as follows:



In addition to 1-nitropropane, 3-nitro-2-pentanol, 2-nitropropane, and nitrocyclohexane are good substrates; the enzyme is designated "nitroalkane oxidase" (EC class 1.7.3). The enzyme has a molecular weight of approximately 185,000 and consists of four subunits identical in molecular weight (47,000). Flavine adenine dinucleotide was required for the enzyme activity and could be replaced in part by riboflavine 5'-phosphate. The maximum reactivity was found at about pH 8.0. The enzyme was inhibited significantly by HgCl_2 , KCN, *p*-chloromercuribenzoate, and *N*-ethylmaleimide. The Michaelis constants are as follows: 1-nitropropane, 1.54 mM; 2-nitropropane, 7.40 mM; nitroethane, 1.00 mM; 3-nitro-2-pentanol, 3.08 mM; nitrocyclohexane, 0.90 mM; and flavine adenine dinucleotide, 1.33 μM .

L-Lysine- α -Ketoglutarate ϵ -Aminotransferase. Properties of the Bound Pyridoxal 5'-Phosphate. H. Misono and K. Soda. *J. Biochem.*, **82**, 535 (1977). — L-Lysine- α -ketoglutarate ϵ -aminotransferase of *Flavobacterium lutescens* (*Achromobacter liquidum*) IFO 3084 shows positive circular dichroic bands at 340 and 415 nm where absorption maxima are observed, and fluorescence maxima at 380 and 490 nm on excitation at 340 and 415 nm, respectively. The pyridoxal 5'-phosphate absorbing at 415 nm is bound through an aldimine linkage to an ϵ -amino group of the lysine residue of the protein. Upon aging, the 415 nm pyridoxal 5'-phosphate changes to a less active form (λ_{max} , 325 nm), which is distinguishable from the 340 nm pyridoxal 5'-phosphate. This 325 nm bound pyridoxal 5'-phosphate is reduced with sodium borohydride and shows no circular dichroism. When the semioenzyme is aged under the same conditions, no spectral change is observed. These findings suggest

that the pyridoxal 5'-phosphate bound through an aldimine linkage may be converted into a carbinol amine or some other related form by aging.

Properties of 2-Nitropropane Dioxygenase of *Hansenula mrakii*. Formation and Participation of Superoxide. T. Kido and K. Soda. *J. Biol. Chem.*, **253**, 226 (1978). — 2-Nitropropane dioxygenase, purified to homogeneity from a yeast, *Hansenula mrakii*, is significantly inhibited by superoxide dismutase and various scavengers for superoxide anion such as cytochrome *c*, epinephrine, NADH, thiols, and polyhydric phenols. The reduction of cytochrome *c* and the oxidation of epinephrine and NADH are concomitant with the inhibition of enzymatic oxygenation. Neither the oxidation nor the reduction occurs in the presence of superoxide dismutase or in the absence of 2-nitropropane or oxygen. Superoxide anion added externally induces the oxygenation. These findings indicate the generation of superoxide anion and its participation in the oxygenation of 2-nitropropane.

The difference spectrum of the binding of NADH to 2-nitropropane dioxygenase exhibits a negative peak at 353 nm. One mole of NADH is bound to 1 mol of the enzyme and the *pro-R* hydrogen of the nicotinamide moiety of bound NADH predominantly is transferred to superoxide anion formed enzymatically or given externally. Thus, the diastereotopic hydrogen of NADH is discriminated by the enzyme, although not completely.

Biochemistry of D-amino Acids (I). K. Soda. *Kagaku (Chemistry)*, **32**, 517 (1977), in Japanese. — The occurrence of D-amino acids in microorganisms, higher plants and animals, and their structures and physiological roles are reviewed.

D-amino acids as a constituent of peptide-antibiotics and mode of action of the antibiotics particularly are discussed.

Biochemistry of D-amino Acids (II). K. Soda. *Kagaku (Chemistry)*, **32**, 627 (1977), in Japanese. — Metabolism of D-amino acids, enzymes related to the metabolism and their enzymology are reviewed. The properties and reaction mechanism of amino acid racemases and epimerase are described in detail.

Regulation Mechanism of Vitamin B₆ Enzyme Activity — Kynureninase and Some Other Enzymes — K. Soda, K. Tanizawa, and M. Moriguchi. *Vitamins (Japan)*, **51**, 449 (1977), in Japanese. — L-Kynurenine hydrolase, aspartate 4-carboxy-lyase and arginine racemase can catalyze the transamination between various amino acids and α -keto acids. The activities of these vitamin B₆ enzymes are regulated by this transamination of the coenzyme moiety. Differences between the regulation mechanisms of the three enzymes are discussed.

A Novel Flavoenzyme Catalyzing the Oxidation of Nitro Compounds. K. Soda. *Vitamins (Japan)*, **52**, 172 (1978), in Japanese. — A nitroalkane-oxidizing enzyme was purified from a cell extract of *Hansenula mrakii* grown in a medium containing nitroethane as the sole nitrogen source. Superoxide anion is generated and participates in the oxygenation of 2-nitropropane catalyzed by the enzyme.

Location of the Cooperative Melting Regions in Bacteriophage fd DNA.

H. Tachibana, A. Wada, O. Gotoh, and M. Takanami. *Biochim. Biophys. Acta*, **517**, 319 (1978). — Differential melting profiles of the linear replicative form (RF-III) DNA of bacteriophage fd, of the fragments obtained by the restriction endonuclease *Hin*H1 and of those obtained by *Hga*I were investigated. With these results a physical map which locates the cooperative melting regions on the DNA was constructed, and compared with the genetic map.

Recognition Sequence of a Restriction Endonuclease from *Haemophilus gallinarum*.

H. Sugisaki. *Gene*, **3**, 17 (1978). — From comparison of the sequences in and around the cleavage sites of restriction endonuclease *Hga*I isolated from *Haemophilus gallinarum*, it was found that this enzyme recognizes a specific but asymmetric penta-nucleotide sequence, GCGTC, and introduces staggered cleavages at appoint positions away from the recognition sequence, generating protruding 5'-ends of five nucleotides. The sequences surrounding the cleavage sites bear no obvious relation to one another. This enzyme is therefore very useful for the construction of the accurate cleavage map of a DNA molecule, because it is possible to identify adjacent fragments from their 5'-terminal sequences.

Isolation and Characterization of Transducing Coliphage fd Carrying a Kanamycin Resistance Gene.

N. Nomura, H. Yamagishi, and A. Oka. *Gene*, **3**, 39 (1978). — The DNA segment (Tn903) with a size of 3,100 nucleotide pairs which carries a gene specifying kanamycin resistance derived from a chimeric plasmid pML21 was transposed to various sites on the filamentous phage fd DNA. Wild type fd can be restored by excision of Tn903 from the resulting hybride DNA molecule. The fd DNA carrying Tn903 when converted to the mature phage particle, was capable of transducing the kanamycin marker, and its replicative form DNA could be maintained in a bacterial cell like a plasmid.

Fine Cleavage Map of a Small Colicin E1 Plasmid Carrying Genes Responsible for Replication and Colicin E1 Immunity.

A. Oka. *J. Bacteriol.*, **133**, 916 (1978). — A small plasmid (pA02, 1 mega-dalton) carrying genes responsible for replication and colicin E1 immunity was constructed from colicin E1 plasmid by using an *in vitro* recombination technique. pA02 DNA was further cleaved into unique fragments with seven restriction endonucleases, and a fine cleavage map was constructed. This made it possible to analyse the gene structure of this plasmid in the sequence level.

Sequence and Regulatory Signals of the Filamentous Phage Genome.

H. Schaller, E. Beck, and M. Takanami. *The Single-stranded DNA Phages* (ed. D. T. Denhardt, D. H. Dressler, and D. Ray), Cold Spring Harbor Lab. Press, New York, pp. 139-163 (1978). — The entire sequence of the male-specific filamentous phage fd (6,380 bases) has been determined in this laboratory in collaboration with H. Schaller's group of University of Deidelberg. In this article, regulatory regions were assigned on the sequence of this phage and presented together with the sequence data.

Solid-Phase Syntheses of Glu₂₀Ala₂₀Phe and Ala₂₀Glu₂₀Phe by the Step-by-Step Coupling of Dipeptide and Tetrapeptide. S. Takahashi. *Bull. Chem. Soc. Japan*, **50**, 3344 (1977). — The title compounds were synthesized by the step-by-step coupling of BOC-derivatives of Ala-Ala and (γ -Bzl-Glu)₄ to phenylalanyl resin using dicyclohexylcarbodiimide. The products were cleaved from the resin with hydrogen bromide in acetic acid and purified by gel filtration, followed by DEAE-cellulose chromatography, with yields of approximately 10% for both of the hentetracontapeptides. The optical purities of the glutamic acid and alanine incorporated in the peptides were estimated as less than 5% from the analysis of the diastereometric mixture of dipeptides derived from the reaction between the total acid hydrolyzate of the peptides with the *N*-hydroxysuccinimidyl ester of BOC-L-Leu.

Utilization of Computer for Determination of a Nucleotide Sequence. T. Ooi and K. Nishikawa. *Bull. Inst. Chem. Res., Kyoto Univ.*, **56**, 93 (1978). — In the determination of a nucleotide sequence, RNA is digested into fragments by RNase T₁ and A, which have different specificity. The sequence may be determined by arranging the fragments in the correct order and the connecting informations are supplied by the digests with RNase of different specificity. A computer may be utilized for the search of all the ways to arrange the fragments according to the given informations. The results show that, for a RNA of a length of about 100 nucleotides, the set of fragments of both digests are usually not enough to give the unique sequence, and further data on partial digests give rise to the only one sequence. This method, although now classical, may be useful for the determination of nucleotide sequences where new techniques are not applicable.

Effects of Salts on the Stability of Maleylated Tropomyosin. Y. Kubota, M. Oobatake, S. Takahashi, and T. Ooi. *Bull. Inst. Chem. Res., Kyoto Univ.*, **56**, 104 (1978). — Tropomyosin, a typical fibrous protein which has almost 100% α -helix, takes a random coil conformation when lysyl residues are maleylated. This conformational change is due to the increase in charge repulsions between negative charges produced by maleylation. When KF is added to MTM solutions, the recovery of α -helix can be observed by the decrease of ellipticities at 222 nm and 208 nm of circular dichroic spectrum (CD). Therefore helix-coil transitions induced by heat on the salt-induced α -helix were measured by CD measurements. Thermodynamical quantities, transition temperature, T_m , enthalpy and entropy of the transition were obtained by the analysis of the transition curves using a curve-fitting technique at various salt concentrations (C_s). The results show that T_m increases with the increase in C_s , with a linear relation between T_m and $\ln C_s$. It is inferred from this result that MTM behaves like a polyelectrolyte, and the major origin of the salt effect is the shielding of charges by small ions to reduce the electrostatic free energy.

A Circular Dichroic Spectral Study on Disulfide-Reduced Pancreatic Ribonuclease A and Its Renaturation to the Active Enzyme. S. Takahashi, T. Kontani, M. Yoneda, and T. Ooi. *J. Biochem.*, **82**, 1127 (1977). — Disulfide-reduced RNase A, which could be reoxidized to give the native enzyme, was shown

to have a CD spectrum quite different from that of the native enzyme or a random coil. Disulfide-reduced and fully cysteine-S-carboxamidemethylated RNase A was used for further CD-spectral analysis instead of unstable reduced RNase A because the derivative was stable and gave a spectrum identical to that of reduced RNase A. Curve-fitting analyses showed the presence of 14% α -helix and 25% β -structure in this open chain derivative of RNase A. The time dependence of CD spectra during the oxidative renaturation of reduced RNase A was analyzed and changes in α -helical and β -structure contents during the reaction were estimated. It was shown that the change in the content of β -structure was slower than that of α -helix content and approximately paralleled the appearance of the enzymatic activity.

Sodium Borohydride as a Reducing Agent for Preparing Ninhydrin Reagent for Amino Acid Analysis. S. Takahashi. *J. Biochem.*, **83**, 57 (1978). — Sodium borohydride, in place of stannous chloride or titanous chloride, is effective in the preparation of the ninhydrin reagent for automated amino acid analysis. The reagent, coupled with dimethyl sulfoxide as a solvent, afforded a very stable ninhydrin solution which did not form precipitates in the flow lines of the analyzer.

Tropomyosin Fragments Obtained by Tryptic Digestion. H. Ueno and T. Ooi. *J. Biochem.*, **83**, 1423 (1978). — Trypsin-resistant fragments obtained by the digestion with trypsin of rabbit skeletal tropomyosin were separated into the precipitate and supernatant fractions at pH 4.3 in 1 M KCl. SDS-gel electrophoresis showed 16,000 and 14,000 dalton bands for the supernatant (*s*-fragment) and an 11,500 dalton band for the precipitate (*p*-fragment). The *p*-fragment had the same C-terminal portion as intact tropomyosin, and could form an intra-chain disulfide bond on oxidation. Therefore, this fragment was deduced to be polypeptides from some point on the N-terminal side of Cys 190 to the intact C-terminal. The *s*-fragment, on the other hand, did not contain any cysteine, Phe or His residues according to amino acid analysis, suggesting that the fragment is derived from the N-terminal side from Cys 190. The *p*- and *s*-fragments appear to be in coiled-coil form in solution, having α -helical contents of 77 and 71%, respectively and are able to interact with intact tropomyosin. The *s*- and *p*-fragments have little binding capacity individually to troponin, but the mixture showed clear binding with troponin independent of Ca^{++} in solution as detected by gel electrophoresis. From these results, it can be inferred that the troponin binding regions in tropomyosin are located on both sides of Cys 190, where trypsin attacks more easily than at other parts of the molecule.